Schnepf *et al. Microplastics and Nanoplastics* (2023) 3:16
https://doi.org/10.1186/s43591-023-00064-4

Microplastics and Nanoplastics

REVIEW

Open Access

A practical primer for image-based particle measurements in microplastic research

Uwe Schnepf[1*], Maria Anna Lioba von Moers-Meßmer[1] and Franz Brümmer[1]

Abstract

Microplastics have been detected in large numbers around the world. Not only their sheer number threatens ecosystems, their biodiversity, and human health, but risks are also posed by particle characteristics such as size and shape. However, at the moment their measurement is neither comprehensive nor harmonized, making the data ineligible for risk assessment. To change this, we propose an image-based workflow, whose six steps are oriented to international guidelines and lessons learned from more developed research fields. Best practices for sample preparation, image acquisition, and digital image processing are reviewed to assure accurate and unbiased particle measurements. On behalf of this, we selected metrics to quantitatively characterize both size and shape. The size of microplastics should be estimated via the maximum Feret's diameter. Particle shape can be measured via shape descriptors, for which we derive harmonized formulas and interpretation. *Roundness*, *solidity*, and *elongation* were selected by applying hierarchical agglomerative clustering and correlation analysis. With these three shape descriptors, all currently charaterizable dimensions of particle shape can be measured. Finally, we present actions for quality control as well as quality assurance and give recommendations for method documentation and data reporting. By applying our practical primer, microplastic researchers should be capable of providing informative and comparable data on particle characteristics. From this improved data, we expect to see great progress in risk assessment, meta-analyses, theory testing, and fate modeling of microplastics.

Keywords Microplastics, Particle measurement, Static image analysis, Particle size, Particle size distribution, Particle shape, Shape descriptors, Risk assessment, Harmonization

Introduction

Plastic littering gained tremendous attention in both, science and media. In the past decade, a special focus was laid on plastic particles [1]. If these have a size between 1 to 1000 or 5000 µm in their longest dimension, then they are called microplastics [2–4].

For this novel entity, mankind is currently operating outside the planetary boundaries [5]. As a result of the constant littering and transport of plastic pollution, a plastic cycle has been established on a global scale [6]. The worldwide exposure with microplastics negatively affects biota [7–9], human health [10], and climate [11]. They also possibly influence biogeochemistry [12] as well as soil properties [13–16]. Furthermore, plastics get incorporated into new geological formations [17–19]. Even with an immediate halt of plastic littering, it is suspected that the toxicological effects could become even greater, because the high persistence of plastics has created a global plastic toxicity debt [20–22].

But microplastics are not just number concentrations [23], they are also a diverse contaminant suite [24]. Consequently, two samples comprising of the same number of microplastics may have totally different ecological impacts [25]. It has already been demonstrated for a variety of particle characteristics that they are causative

*Correspondence:
Uwe Schnepf
uwe.schnepf@bio.uni-stuttgart.de
[1] University of Stuttgart, Institute of Biomaterials and Biomolecular Systems (IBBS), Research Unit Biodiversity and Scientific Diving, 70569 D-Stuttgart, Germany

factors for toxicity [26, 27]. Thus, a comprehensive particle characterization was recently recommended by two international groups of experts [28, 29].

Since microplastics are polydisperse by definition [3, 4] and size has also the highest biological concern to aquatic organisms [30], it is obvious to measure size by default. Although particle size measurements appear simple at first glance, there are many methodological pitfalls. For example, a lot of studies do not even specify which metric was used to characterize size [31]. And even when these methodological details are available, different size metrics are reported, making comparability between studies very difficult or even impossible in some cases. Furthermore, the particle size distribution resulting from the measurement is mostly inadequately visualized [31, 32]. Hence, harmonization and higher reporting standards are urgently needed.

The same criticism applies to the measurement of particle shape, which also accounts for the environmental impact of microplastics [26, 27]. The shape of microplastics is mostly characterized by categories which, however, differ considerably between studies [33]. Hartmann and co-workers [4] harmonized them by defining four shape categories: roundish particles are called spheres, microplastics of irregular shape are now labeled as irregular particles, particles with a high length-to-diameter ratio are named fibers and planar plastic items are termed films. Recently, Liu and co-workers have expanded this categorization. Based on expert interviews, they proposed nine categories to describe particle shape: fiber, rod, ellipse, ovoid, sphere, quadrilateral, triangle, free-form, and unidentifiable [34]. Yet no qualitative shape categorization can ever characterize the continuum of particle shape [35]. Hence, shape must be measured quantitatively. For this particle shape measurements of microplastics, shape descriptors were previously proposed as the optimal metric [29, 36].

Indeed, size and shape are only two out of many particle characteristics of microplastics. Nonetheless, both are important drivers of microplastic toxicity [26, 37]. Consequently, particle characterization needs to provide data on size and shape of microplastics simultaneously.

Particle measurements are mostly conducted by sieve fractionation and static image analysis. However, sieve fractionation is not suitable for a comprehensive characterization of microplastics, as particle shape measurements are not possible with this method and data on size is often ineligible for risk assessment [32].

Thus, our review is going to be focused only on static image analysis. One major advantage of this method is that a microscope is employed. It is the only instrument that allows the simultaneous observation and measurement of both, size and shape for an individual plastic particle [38–40]. Microplastics > 10 µm can be characterized by light microscopes coupled with Fourier-transform infrared spectroscopes (FTIR) and Raman spectrometry, the two most popular techniques for the identification of environmental microplastics [41]. An in-depth discussion on suitable analytical methods that characterize submicron plastics and nanoplastics is provided elsewhere [39]. It was often argued that microscopy is not the best method for particle characterization [39], while laser diffraction is often considered as the gold-standard. Nonetheless, static image analysis can be comparably accurate, if strict quality control and quality assurance measures have been implemented [42]. Overall, this proves that static image analysis is a convenient and reliable method for particle characterization.

Details on materials and methods are often sparsely reported in case of particle measurements [31]. In some studies, no particle measurement is even performed at all. We suspect that the previously mentioned methodological deficiencies are related to the fact that microplastics research is interdisciplinary and, thus, many scientists simply have not had sufficient training in the comprehensive characterization of particles. Therefore, the objective of this review is to teach the basics of particle measurements by introducing a workflow that incorporates the following six steps: i) subsampling of microplastics from the bulk, ii) image acquisition by light microscopy, iii) processing of digital images, iv) measuring particle size and shape descriptors, v) quality control and quality assurance, and vi) data reporting (Fig. 1). We will now provide a practical primer on each step by integrating international guidelines and lessons learned from powder technology, pharmaceuticals, natural sediments, and nanomaterials.

Step 1: sample preparation

Before microplastics can be characterized, samples need to be carefully prepared (Fig. 1). While this step is essential for the overall quality of the particle measurement [43], the method is completely different depending on the type of study.

With effect studies, the bulk of microplastics is stored in containers or bags. From these, subsamples are then taken for particle measurement. This is also the typical method in powder technology, on which this step will be focused.

In contrast, when environmental matrices are monitored for microplastic pollution, it is common practice to harvest the extracted particles on special sample holders for spectroscopic identification. Therefore, many methods of sample preparation, which are standard in powder technology, are not integrated into the workflow here. Nonetheless, also in monitoring studies, the behavior of

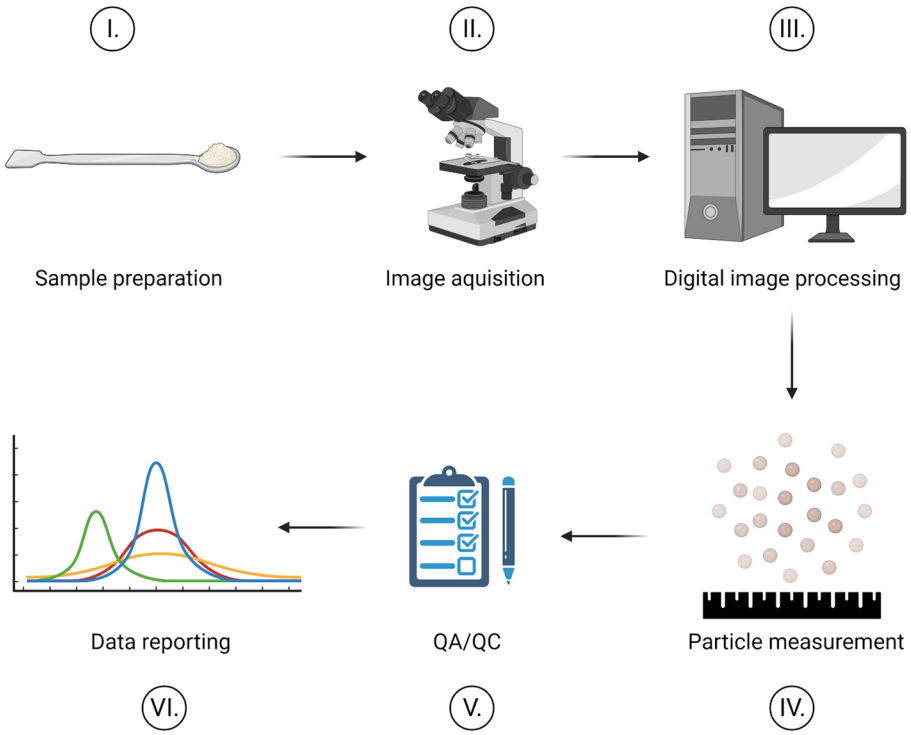

Fig. 1 Workflow for an image-based particle measurement of microplastics. Firstly, at each measuring point a sample is prepared that is uncontaminated, sufficiently large, and representative. Secondly, high-resolution images are then acquired with a calibrated light microscope using appropriate settings. Thirdly, digital image processing is employed to completely separate the microplastics from the background. Fourthly, a multitude of metrics are measured for the characterization of size and shape. Fifthly, the quality of the measurements is controlled and assured (QA/QC) by checking for any source of bias. Sixthly, frequency distributions and summary statistics of size and shape are reported in a comprehensive and comparable manner. Created with biorender.com

single microplastics in a particle collective, the specifics of static image analysis, and the implications of both on the minimum number of particles are in part relevant to the accuracy of particle measurement and, consequently, to sample preparation.

Before we review best practices for sample preparation of microplastics that are used in effect studies, we would like to first briefly consider the different mixture types of polydisperse particle collectives. Then, we summarize the advantages and disadvantages of common subsampling methods, give recommendations on the minimum number of particles, implement actions to reduce contamination, and discuss at which stages of a study the microplastics should be measured (Table 5).

Mixture types of polydisperse particle collectives

Polydisperse particle collectives can be mixed in several ways. One of the aims of the sample preparation is to optimize the mixture of the bulk in such a way that all microplastics have the same probability to be measured. Only then does the subsample represent the whole multitude of chemical and physical properties of the particles in the bulk. This is the case for perfect mixtures and randomly distributed microplastics.

In a perfect mixture, particles of any size and shape are evenly distributed in the bulk. In practice, however, it is impossible to have this type of mixture [43].

But through careful sample preparation, it is possible to obtain a random distribution in the bulk. Although the microplastics are not evenly distributed in this type of mixture, the probability of being sub-sampled is the same at any location in the bulk [43]. The prerequisites for this are that the subsample is sufficiently large and that a possible segregation of the bulk has been reversed.

When transported and stored, microplastics always segregate, a phenomenon also known as muesli or Brazil nut effect. Segregation causes smaller particles to migrate to the bottom of the bulk, while the larger microplastics are left at the top. The extent of segregation strongly depends on size, shape and density [43]. The greatest extent occurs with spherical microplastics larger than 50 µm, whereas irregular microplastics smaller than 30 µm hardly segregate at all. In the case of milled microplastics, which are produced for effect studies, a certain extent of segregation can be expected, since their particle

size distribution is very broad and a multitude of shapes are present in the bulk [44]. Hence, if no actions are taken against segregation, a non-representative subsample may be taken.

But even if subsamples are representative, particle measurements can be biased as a result of aggregation [45].

Agglomerates are the result of interactions between particles. They can be formed during storage and by touching or overlapping of microplastics at the sample preparation. The smaller the microplastics, the higher the potential for aggregation [45]. Since these aggregates do not equal individual microplastics in either size or shape, the measurement of both characteristics may be biased.

Subsampling microplastics from a bulk for particle measurements

Generally, every mixture of microplastics can be randomized by applying an appropriate subsampling method. For environmental microplastics, subsampling methods have been extensively reviewed by other authors [46–49] and, thus, there is already some degree of harmonization in monitoring studies. On the contrary, most effect studies provided only a vague report on the methods used for subsampling, if any [31]. Therefore, we will only focus on how to subsample microplastics from a bulk in the following. Note that this method should not be confused with the preparation of subsamples for ecotoxicity testing itself [50]. Based on our own experiences, we speculate that in the case of a particle measurement, researchers typically use very simple methods for subsampling, e.g., scooping.

Although scooping is easy to implement, this method is very error-prone and comes with many drawbacks [51]. Firstly, only small portions (typically a few milligrams) and not the whole bulk pass through the sample preparation [45].

Secondly, because operators decide where to scoop microplastics in the bulk, particle measurements can be biased due to an operator error. To reduce the operator bias in scooping, microplastics should always be mixed beforehand. Note that shaking and stirring should not be applied, because this method forces small microplastics to the bottom. Alternatively, methods from sedimentology can be easily adopted to sample microplastics from the bulk. Here, the gold-standard for the sampling of polydisperse particle collectives are splitting methods, e.g., coring and drilling [29]. They minimize segregation, ideally leading to a random distribution of particles.

No matter which method is chosen for subsampling, the microplastics that are getting sampled for particle measurement have to come from the same bulk as the particles applied in the ecotoxicologial experiment [45].

In order to account for potential heterogeneity in the bulk, it is recommended to take several subsamples and to check their measurement errors (Outlier detection in subsamples). For particle size distributions of microplastics, it was shown that the relative standard deviation of the particle counts within a size interval can even exceed 100% [42]. ISO 14488:2007 recommends to take at least ten subsamples by scooping, which are pooled after step 5, which is quality control and quality assurance [51]. Note that these subsamples should all have approximately the same weight [51].

Subsampling methods should also aim to de-agglomerate microplastics, because the measurement of single particles is a prerequisite for an accurate characterization [52]. Although several methods have been developed for de-agglomeration, e.g., ultrasonification, none of them permanently change the conditions under which agglomerates formed during storage. Thus, after a certain time, the particles will re-agglomerate. Agglomeration can only be minimized to a very small degree. One method is to drastically reduce the sample mass, which decreases the rate at which microplastics agglomerate when they are sprinkled on the microscope slide [53]. The sprinkling itself ought to be optimized by passing the scooped microplastics through a sieve with meshes that are slightly larger than the largest particle [54]. Hereby the number of touching and overlapping microplastics is further minimized. Noteworthy, the extent of agglomeration cannot be determined quantitatively. That is because even for trained operators, it is almost impossible to distinguish larger microplastics from agglomerates with a microscope [45]. Instead, the extent of agglomeration can be estimated by comparing particle size distributions obtained by different measurement techniques [45].

Minimum number of particles

Given the polydispersity of microplastics [38, 55], agglomeration, the drawbacks of subsampling methods, and other factors, an accurate characterization requires the measurement of a very large number of microplastics.

For a static image analysis, one crucial factor is the particle orientation, as this is random [56]. When microplastics are sprinkled on top of a microscope slide, they typically attain the most stable particle orientation. However, especially for irregular particles, many different stable particle orientations exist. Therefore, even if all microplastics have the same size and shape, measuring that size and shape will not result in one but several different values [57]. In order to estimate the true value for an individual particle as accurately as possible, a large number of microplastics need to be measured.

To compromise between the aimed accuracy and the effort to obtain this, a minimum number of particles

must be determined as part of the sample preparation. Recommendations range from 100—14,000 particles for the measurement of size [55, 58]. This is much higher than the recommendations for an accurate polymer identification of environmental microplastics, i.e., 125 microplastics in the size fraction > 100 µm [47]. Unlike plastic types, which are comprised of only a few tens of polymers, size and shape are wide-ranging continua [35].

Consequently, the width of their distributions strongly influences the minimum number of particles [52]. Generally, the broader the particle size distribution, the larger the proportion of the bulk that needs to be measured to reach a given accuracy, especially for the upper tail, where counts are low [52]. Very broad particle size distributions were reported for both environmental [35, 59, 60] and milled microplastics [44]. Therefore, it is best to orientate oneself towards the upper range of the recommendations.

However, this cannot be generalized. It is advisable to determine the minimum number of particles for each particle collective individually. For this, various methods have been developed.

According to ISO 13322–1:2014, the minimum number of particles is the one at which the mean particle size can be measured with a certain accuracy given a specified probability [52]. For instance, the size of 10,000 microplastics needs to be measured to have a relative standard deviation of 1% [38].

The value stabilization method tests at which number of particles the mean or the standard deviation stabilizes [40]. Usually, the mean stabilizes faster than the standard deviation [55]. This method can be applied for distributions of either size or shape.

Another methods is based on the Chi-square goodness of fit test [58]. Here, the distribution from an increment of the data on size or shape is fitted to the distribution of the whole sample. If this is successful for two increments in a row, the second of these increments is set to be the minimum number of particles. This figure is often considerably smaller than for other methods.

The selection of an appropriate method is mainly influenced by which statistical property is to be controlled, i.e., accuracy, mean and standard deviation, or the overall distribution. All methods require either experience from former studies or a pilot. If no information on the particle characteristic of interest can be derived beforehand, as a rule of thumb, at least 300 environmental microplastics and 10,000 milled microplastics should be measured [55]. However, more studies should be conducted to establish such general recommendations.

As not all particles can be accepted for particle measurement, the number of measured microplastics should always exceed the minimum number of microplastics [52].

Contamination

Subsamples of microplastics, which are designated for particle measurement, have to be protected from contamination through any other particulate source [51]. Consequently, all instruments ought to be cleaned prior to usage and the sample holders should be covered throughout the subsequent image acquisition [45]. To minimize the contamination by airborne microplastics, counter actions need to be implemented in each part of the sample preparation [46, 61–64].

Measuring points

For microplastics, the state of dispersion depends on the conditions in the respective environment [45]. For example, aggregates are formed when microplastics are introduced into aqueous solutions [65]. This indicates that the distributions of size and shape may be fundamentally dissimilar at different stages of a study.

Hence, in an ecotoxicological experiment samples shall be taken at four measuring points [45]: i) after production of microplastics, ii) during exposure, iii) when microplastics were ingested by the organisms, and iv) post mortem or at the end of the experiment, depending on the response (Fig. 2).

It is particularly important to characterize the distributions during exposure. Firstly, this is because the greatest alterations in dispersion are to be expected at this stage. Secondly, this stage determines which proportion of the microplastics are bioavailable [66]. However, measuring microplastics during exposure is challenging, especially in complex matrices, e.g., soil. In particular, static image analysis is inapplicable during exposure [45]. Particle characterization in vivo and post mortem is best done qualitatively by microscopic analysis [45]. To better visualize microplastics in vivo, they can be labeled by the fluorescent dye Nile red [67–69]. With this method, however, there exists a large set of analytical challenges. For instance, as Nile red can leach out, it might be mistaken with microplastics in animal tissue [70].

The state of dispersion needs to be considered in monitoring studies, too. Here, the extraction of microplastics is a complex procedure, where a large variety of salt solutions and enzymes are used [63, 71]. Thus, it is very likely that particle measurements at the end of this procedure may not resemble the distributions of size and shape in situ.

We therefore stimulate the development of novel methods that can facilitate particle measurements directly in the environmental matrix. As long as no such method is available, it should always be considered that the

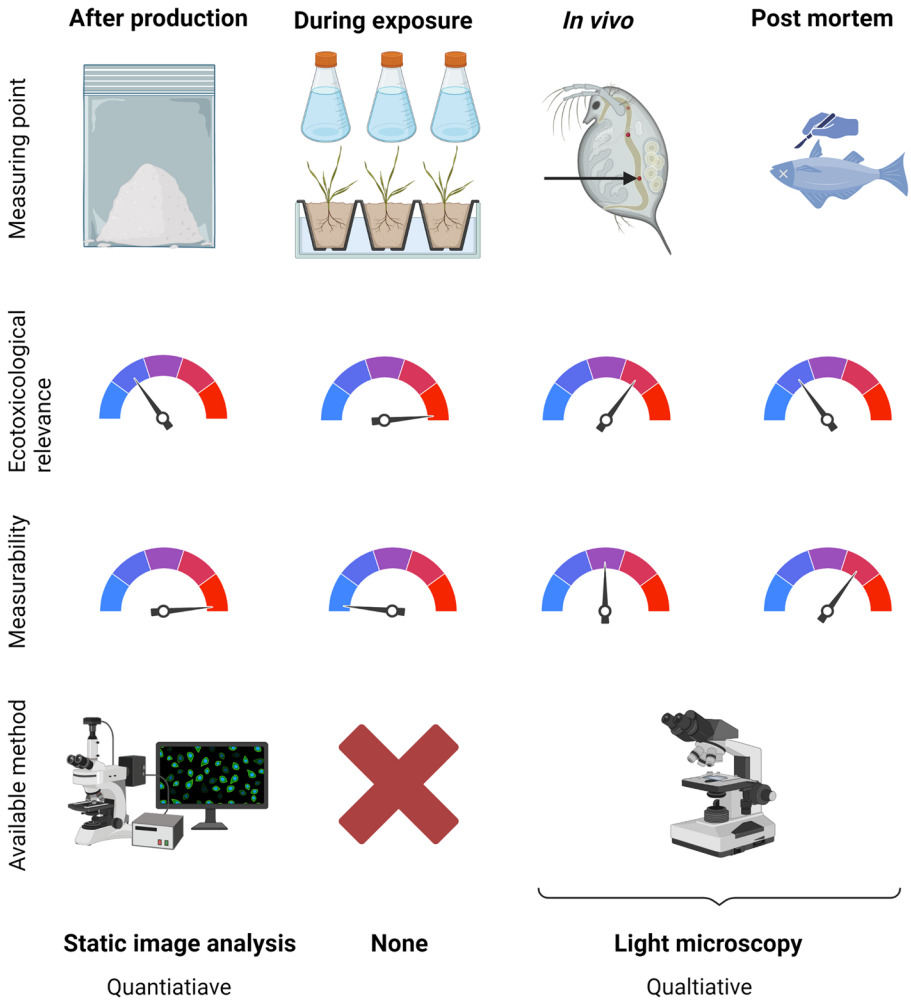

Fig. 2 Measuring points at which microplastics should be measured in an effect study. After production, the measurability is very high, but the ecotoxicologial relevance of the data on size and shape is little. Note that the same criticism applies to particle measurements of microplastics that have been extracted from environmental matrices. During exposure, the state of dispersion might change and, consequently, bioavailability. Unfortunately, no methods are available for particle measurements at this important stage. In vivo and post mortem, microplastics can be characterized at least qualitatevily via light microscopy. Created with biorender.com

measured distributions of size and shape might be dissimilar from those during exposure, in situ, and in vivo.

Step 2: image acquisition

For the measurement of the microplastics in the samples, a light microscope is used to acquire digital images (Fig. 1).

To take high-quality images, calibration, microscope settings, and image storage need to be taken into account (Table 5). Especially, magnification, illumination, and focus must be the same before and after image acquisition [52]. All microscope settings must be carefully documented in order to guarantee reproducibility [72]. Note that our recommendations for adequate microscope settings might be also relevant for the visual identification of environmental microplastics, were particles smaller than 50 µm cannot be identified so far [73].

Yet it requires not only high-quality images, but it is also necessary to image a sufficient number of fields of view to achieve the minimum number of particles.

Calibration

Trough calibration, a scale is gotten for the conversion of pixels into physical size units. It is best done by imaging a certified graticule with the same microscope settings (magnification, illumination) as will be employed for the particle measurement [52]. To detect possible distortions, both the x and y plane should be calibrated [52].

On the image of the certified graticule, a specified length is measured ten times at different positions [74].

Ultimately, the scale is reported as the average of these ten measurements. In addition, this method makes it not only possible to estimate the measurement error via the relative standard deviation, but also to detect spherical abberations of the lens [43].

Magnification

The magnification is chosen according to the smallest plastic particle in the sample [52]. A proper choice assures that the pre-defined measurement accuracy can be reached for all microplastics and that every particle is detected by the camera [75, 76].

Theoretically, the whole size range of microplastics can be measured via light microscopy, as the theoretical detection limit of this method is 0.2 µm. However, it is often not possible to image particles smaller than 0.8 µm under realistic conditions [40]. In practice, it has also been evident that microplastics smaller than 3 µm should not be measured with a light microscope [38]. Below that size, the accuracy of the particle measurement is very low, because a diffraction halo around the microplastics occurs. This leads to an overestimation of size and also to an inaccurate measurement of shape (c.f. Equation (3).

In order to accurately measure all microplastics, a rule of thumb says that the smallest particle of interest ought to be represented by at least five to ten pixels. This typically requires a very high magnification.

Certainly, if the field of view is comparatively small, highly magnifying a particle collective can result in a low sensitivity for large microplastics [77]. To overcome this drawback, large montages of several small images should be acquired with a motorized stage.

Illumination

Illumination has an influence on which is the smallest measurable size and also on the contrast. In general, Köhler illumination should always be employed to assure a uniform illumination over the whole field of view.

The type of illumination should be chosen based on the smallest size of interest and the particle shape. Reflected light should be utilized for microplastics larger than 5 µm, while a light microscope operated in transmission mode with monochromatic light is to be preferred for the measurement of microplastics smaller than 3 µm [40]. For pellets, it was recommended to utilize either top light or light that comes from 45° from the top light position [78].

The contrast should be maximized by adjusting the light intensity optimally [52]. Because if the light intensity is too high, a poor contrast will be the result [43]. Conversely, if it is too low, this will lead to troublesome diffraction at the edges of microplastics [43]. The optimum approach would be to exploit the entire dynamic range, whereby clipping must be avoided [79].

Depth of focus

One of the major drawbacks of static image analysis is the shallow depth of focus of light microscopes [40].

This is especially noticeable at high magnifications. Here, only a small part of the microplastics are in focus. For a given magnification, the maximum range of sharply displayable particles is of factor 30 [43]. As particle size distributions of microplastics are usually very broad, this means that especially larger particles are out of focus.

To overcome this issue, images should be acquired as Z-stacks, because this method allows to achieve any desired depth of focus [80].

Image storage

The bit depth of an image determines the amount of information a computer algorithm gets for digital image processing [81]. Generally, the higher the bit depth, the better. Images should be at least stored as 8-bit grey scale images, while the optimum would be to have 32-bit RGB color images. However, higher bit depths come with the downfall of higher memory requirements and, consequently, much longer computation times. As a compromise, microplastics should be measured on 16-bit grey scale images [79].

Digital images ought to be stored as uncompressed files in the Tagged Image File Format (TIFF). Note that any kind of compression can reduce the resolution of the image, resulting in an undesirable deterioration of measurement accuracy [52]. Images in the format of the Joint Photographic Experts Group (JPEG) are inadequate for particle measurements as well, since the underlying computer algorithm alters the intensity and arrangement of pixels [79, 82].

Number of field of views

How many field of views should be imaged, depends on the pre-set mininum number of particles. The number of field of views can be easily estimated by counting the microplastics in the first images of the measurement series. Here, a buffer should be taken into account, since not all microplastics can be measured inside a field of view ([52], c.f. Measurement frames). The number of microplastics per field of view should be between 5 to 50, as this minimizes the extent of overlapping particles [43].

Step 3: digital image processing

Light microscopy was used to acquire images of the microplastics to be measured. These digital images are, technically speaking, an array of quadratic pixels. An intensity is assigned to each of them based on the

lightness of the sample at the corresponding location. For instance, in an 8-bit grey scale image, these intensities range from 0—255 [81]. Thus, digital images are data and should be treated as such [82]. This data can be utilized for the measurement of microplastics, but therefore the projection of microplastics first needs to be separated from the background (Fig. 1).

For the purpose of this separation, digital image processing offers a variety of computer algorithms, which are subdivided into grey image processing, segmentation, and binary image processing [52] (Table 5). Importantly, the whole separation procedure must not introduce any extra error [52]. Of course, that is best achieved by minimizing the processing of digital images itself, which in turn requires high-quality microscope images [43]. For segmentation, we will empirically show how different computer algorithms affect the results of particle measurements. As a consequence, a detailed documentation of the applied computer algorithms and the belonging software is essential [36, 83].

Grey image processing

As image acquisition is imperfect to some extent, it may be necessary to correct some properties of a digital image. Firstly, they need to be converted to 8-bit, since most computer algorithms for correction have been developed for this bit depth. Since 8-bit images display only a grey scale, this part of the procedure is called grey image processing. Most often, the intensities are to be smoothed and the contrast between the background and microplastics has to be maximized. Ultimately, grey image processing serves to simplify the segmentation, but it may also bias the particle measurements [55].

Smoothing

Smoothing aims to eliminate slight differences in the intensities of neighboring background pixels. Filters are typically applied when point noise is present in the image, whereas background subtraction corrects for uneven illumination [79].

Filters cancel noise by recalculating the intensity of a given pixel based on the intensity of its neighbors [84]. Their number is specified by the size of the filter matrix. The larger the filter matrix, the larger the extent of change in a pixel [81]. If the filter matrix is too large, very small microplastics or thin fibers may be inadvertently removed from the gray scale image [79]. A large variety of filters have been developed, of which we will briefly introduce the most popular ones here. Gaussian filters are frequently applied to smooth an image, but can shift or distort the edges of microplastics [79]. The mean filter replaces the intensity of a pixel with the average intensity of the neighboring pixels [84]. A disadvantage of this computer algorithm is that one outlier can greatly affect the outcome. In addition, a mean filter tends to blur the edges of microplastics, a result that lowers the accuracy of particle shape measurements. A more robust alternative is the median filter, that has been designed to remove point noise in the digital image. However, this type of filter rounds corners, which is again problematic in particle shape measurements [79]. Thus, filters, just like all other computer algorithms in digital image processing, should be employed with caution. Generally, we advocate to avoid the application of filters [82]. To reduce noise, the image acquisition should be optimized instead. If this is not enough, a filter can be used as an exceptional solution. Certainly, the type of filter and the size of its matrix ought to be chosen very carefully.

The background should be subtracted in the advent of an uneven illumination [79]. This artifact occurs even with very high quality light microscopes, because detectors are always imperfect and even the best illumination can slightly change during image acquisition, too. To properly perform background subtraction, an image of the background is first required. It has to be taken from the exactly same viewpoint and with an identical illumination as the images utilized for the particle measurement [84]. In practice, an image of the background can be easily obtained by removing the sample holder. Alternatively, the background can also be estimated by polynomial functions that, e.g., resemble a rolling ball or a sliding paraboloid [85, 86].

Contrast

Smoothing of an image alters its pixel intensities and, thus, can lower the intensity differences between microplastics and the background [79]. This can be reversed by altering the contrast, which is defined as the difference between the minimal and maximum intensity [81].

By multiplying the intensity of every pixel by a given factor, the histogram gets broader and, consequently, the contrast increases [81]. For instance, a factor of 1.5 results in a 50% increase of the contrast. Importantly, the contrast must be altered by the same factor in the whole image [87].

As a first iteration, contrast can be altered by applying a modified auto contrast function [81]. In a nutshell, the pixels having the most extreme intensities are set to the theoretical minimum and maximum intensity. Then, all other intensities are linearly stretched over this range of values. If necessary, the user can further adjust the contrast to ease segmentation.

Segmentation

The objective of a segmentation is to separate microplastics from the background. It is considered to be the most

difficult task in digital image processing [84]. Therefore, a large number of different computer algorithms have been developed for segmentation.

Particularly, edge detection and global automatic thresholding have been found to be suitable methods in the context of particle measurement [52]. However, edge detection results in incompletely closed edges of microplastics, which necessitates exhaustive post-processing [52].

Accordingly, we will focus solely on global automatic thresholding. This set of computer algorithms utilize the distribution of the intensities or other image properties to seek for an optimal cut-off [81]. At this value, pixels are binarized into 0 and 1. Ideally, this binarization separates microplastics from the background. In order to achieve an ideal outcome, global automatic thresholding requires images with a high signal-to-noise ratio, which is typically the case for microplastics [36].

For global automatic thresholding, a bunch of computer algorithms exist. In ImageJ, for example, 17 different algorithms for global automatic thresholding are implemented [85]. Simple algorithms determine the threshold via statistical parameters such as the mean [88] or the mode [84]. Another approach is to assume that a certain proportion of the pixels in the image represents the microplastics [89]. However, all of these algorithms only perform properly if the intensities follow a certain distribution [84]. For instance, an accurate threshold can only be determined by the mode if the intensities have a bimodal distribution. Therefore, other algorithms determine the threshold independently of the distribution [81]. Of these, the popular algorithm by Otsu performs well for many different kinds of digital images [90]. But new algorithms are also still under development [91].

Hence, it is often unclear which of the different computer algorithms performs best for a particular image. To support the user in this difficult decision, computer algorithms for global automatic thresholding can be compared qualitatively and quantitatively [91]. This is done in relation to a reference point, which is chosen to be the outermost pixel of a plastic particle. While such a choice introduces a slight operator bias, it also helps to optimize the segmentation for the needs of the subsequent binary image processing as well as the particle measurement itself.

Whatever computer algorithm is chosen for global automatic thresholding, special care must be taken to appropriately segment the microplastics. Otherwise, either over- or under-segmentation will lead to a notable bias in particle measurements [43]. This bias is a function of size, with smaller microplastics being more affected by an inappropriate segmentation [52]. To illustrate the extent of this bias, we here compare the particle size distributions obtained by two different computer algorithms. These were implemented either in FIJI ImageJ [92, 93] or the software of a microscope manufacturer (c.f. Supplementary Information for details).

For the two plastic types, i.e., LDPE and PBAT/PLA, differences in the maximum Feret's diameter were found to be between 16 µm and 8 µm, corresponding to a deviation of 23% and 10% with respect to the value measured by FIJI ImageJ (Table 1). With this software, a higher particle count was also observed.

Therefore, the automatically performed segmentation of the two softwares was examined by comparing the binarized images with the original images (Fig. 3). From this check, it was found that the computer algorithms implemented in the software by the microscope manufacturer mainly did not segment smaller microplastics. As a result, the median particle size was much higher in this case. This illustrates that the choice of computer algorithm can have a considerable impact on segmentation and, consequently, on the accuracy of particle measurements.

Furthermore, unfavorable image properties can also impact the segmentation. In particular, global automatic thresholding performs poor when the background is unevenly illuminated or non-uniform [84]. While uneven illumination can be easily corrected by background subtraction, a non-uniform background is only to be rectified by an optimization of the image acquisition. If this is not feasible, then it might be possible to determine an appropriate threshold by more complex computer algorithms. An overview of these [94] as well as technical details on specific ones, e.g., clustering [95] and convolutional neural networks [96], can be found elsewhere.

Binary image processing

Once the segmentation has separated microplastics from the background, it is sometimes necessary to

Table 1 Comparison of the particle sizes measured either by FIJI ImageJ or the software by a microscope manufacturer. D_{50} is the median of the particle size distribution, *IQR* is the interquartile range, and *n* the number of microplastics that have been accepted for particle measurement

Plastic type	Software	D_{50} [µm]	IQR [µm]	n
LDPE	Microscope manufacturer	86	61	23,085
LDPE	FIJI ImageJ	70	57	27,456
PBAT/PLA	Microscope manufacturer	89	47	25,791
PBAT/PLA	FIJI ImageJ	81	39	26,443

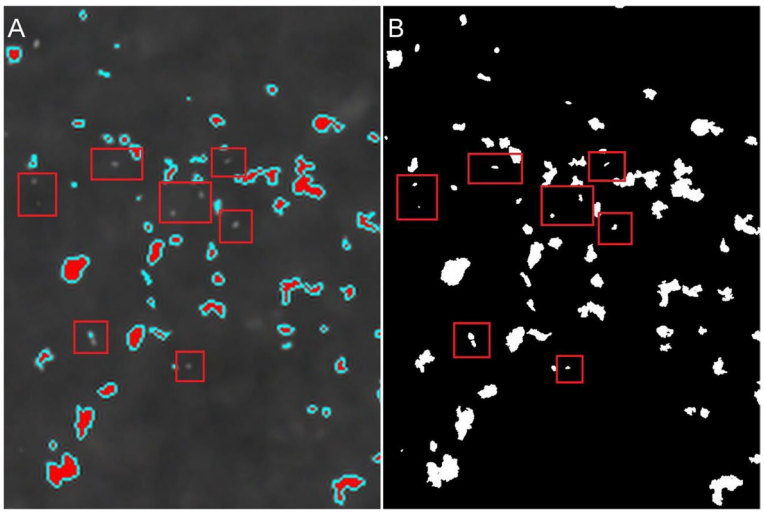

Fig. 3 Comparison of segmenting microplastics and background with different softwares. **A** Global automatic thresholding was applied to binarize the image with the software by a microscope manufacturer. The original image was overlaid with the binary image. Measured microplastics are displayed in red with a turquoise edge. The red boxes mark small particles that were not detected by the computer algorithm. **B** Binary image obtained by global automatic thresholding using the Otsu's computer algorithm in FIJI ImageJ [90]. Microplastics are shown in white. The red boxes mark the same small particles as in the left image, but in this case they were measured by the computer algorithms

further process the binary images. Even with the best sample preparation, touching microplastics are a large source of bias in static image analysis and, thus, they should be separated prior to particle measurement [52].

The separation of touching microplastics is done by morphological filters, i.e., dilation and erosion [43, 81]. Dilation changes white pixels to black, if these white pixels are adjacent to black ones. On the contrary, erosion changes black pixels to white, if these black pixels are adjacent to white ones. In the case where the projection of microplastics is represented by white pixels, this means that dilation enlarges the particle, while erosion leads to a shrinkage. Consequently, both computer algorithms change the size and shape of microplastics [79]. To restore the original size of a plastic particle, the two algorithms are to be combined. Here, opening is the sequence of an erosion followed by a dilation. This allows the separation of touching microplastics. Despite opening, the watershed transformation is also a frequently applied computer algorithm for the separation of touching microplastics [84]. Importantly, classical watershed algorithms were specifically designed for spherical particles [97]. Thus, they are inappropriate for the separation of most microplastics, since the majority of these particles are either fibers or irregularly shaped [98]. Recently, watershed transformation was also developed for irregular microplastics [97]. However, both opening and watershed transformation require to choose the optimal settings manually, which makes these computer algorithms inconvenient for automation and high-throughput analysis.

Although the separation of touching microplastics is technically possible, it should nevertheless be applied with great caution. That is because there is a high chance to decrease the accuracy of particle measurements, especially for irregular microplastics [52]. Hence, ISO 13322–1:2014 recommends to separate only spherical particles and reject all other touching particles from the measurement [52]. However, this recommendation is rather unpractical, as even trained operators can hardly differentiate between two touching microplastics of irregular shape and one large sized plastic particle [45]. Instead, we suggest to reduce the extent of agglomeration in the particle collective as much as possible and to pass the separation of touching microplastics by binary image processing [53, 54].

Dilation and erosion can also be used to fill holes [79]. These holes can be introduced to the projection of microplastics if there are, e.g., reflections on the surface of pellets or transparent particles [55]. Without correction, the projection area and, consequently, size and shape would be biased. This can be easily prevented by filling holes.

The particle size measurement of fibers can also be performed through a special variant of erosion called skeletonization [36]. Here, pixels at the edge of microplastics are removed so long until this would cause the particle to be separated into two parts [79]. The length of the

midline then characterizes the size of fibers (c.f. Geodesic length and width).

Step 4: measurement

Digital processing of the acquired images is now followed by the particle measurement of the microplastics (Fig. 1). First, however, some type of measurement frame is inserted into the image to be certain that only microplastics with an entire two-dimensional projection are characterized. Subsequently, a multitude of size metrics and shape descriptors can be measured for each microplastic individually.

Measurement frames

In a static image analysis, only those microplastics must be measured whose two-dimensional projection represents the entire particle realistically. Accordingly, microplastics that are cut off by the margins of the image shall be omitted. Therefore, in practice, one of three different measurement frames is placed inside the field of view ([52], Fig. 4).

With the first type, just those microplastics are characterized whose centroid lies within the measurement frame (Fig. 4A).

In the case of the second variant, a measurement is carried out only when the two-dimensional projection of a microplastic touches the right or upper margin of the measurement frame (Fig. 4B). On the contrary, all particles touching the left or bottom margin of the measurment will be excluded. Relevantly, there has to be sufficient space between the field of view and the measurement frame. Otherwise it could happen that a plastic particle, which should be measured, is cut off at the image margins and, consequently, this would bias results [52].

Apart from this, the main disadvantage of the two previous types is that microplastics can just be measured in a small part of the field of view. For this reason, many more images have to be acquired to reach the minimum number of particles, which is both laborious and time-consuming.

To avoid such an additional effort, instead of separate measurement frames, it is more convenient to have the third type, which is neglecting all microplastics whose two-dimensional projection touches any margin of the measurement frame (Fig. 4C). Here, the measurement frame can be as large as the field of view itself, as it is impossible that a plastic particle is erroneously accepted for characterization in more than one measurement frame. However, this type has to consider that the probability of cut-off from the margins is inversely proportional to the particle size and therefore the raw counts need to be corrected ([52], c.f. Particle size distributions).

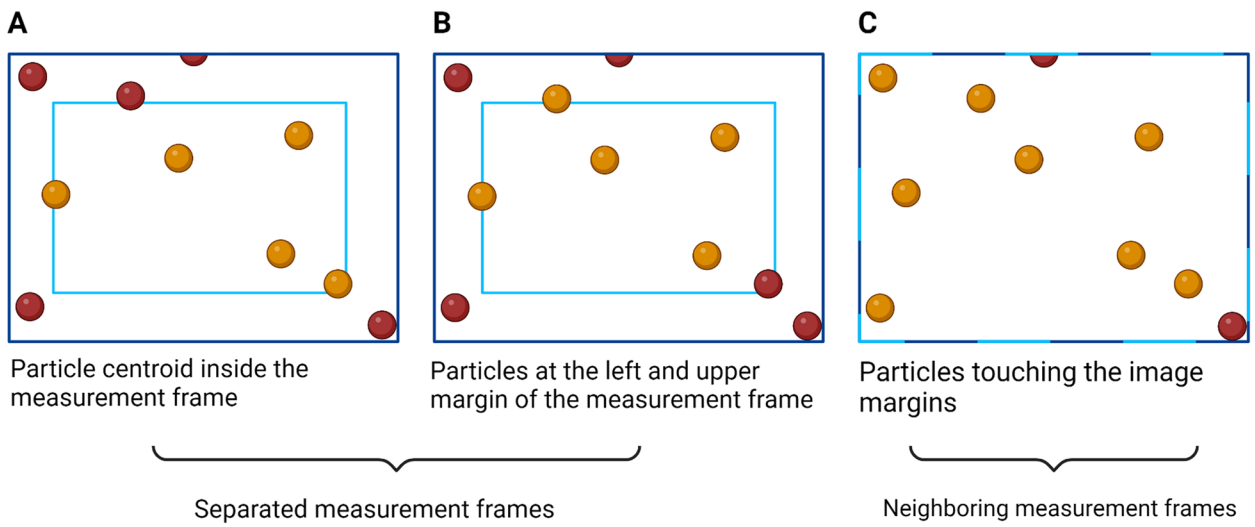

Fig. 4 The three different types of measurement frames loosely based on ISO 13322–1:2014 [52]. Principally, the location of a plastic particle inside a measurement frames defines whether it is measured. The margin of the measurement frame is represented by dark blue, while the margin of the field of view is colored in light blue. Microplastics that are going to be measured are orange, whereas excluded plastic particles are red. **A** Only microplastics whose centroid lies inside the measurement frame are considered for particle size and shape measurement. **B** All particles touching the right and upper image margins are measured, whereas microplastics at the left and bottom are ignored. For both, **A** and **B**, the measurement frames are separated. **C** In the third type, the measurement frames are neighboring, since each measurement frame is as large as the respective field of view. Microplastics that are cut off by the margins are all excluded from particle measurement, which makes it of necessity to correct the raw counts. Created with biorender.com

Step 4a: particle size measurement

Intuitively, the size of particles is characterized by their diameter. But this size metric can only be measured for microplastics that have a regular geometry, such as pellets, films and unknotted fibers [56]. For irregular microplastics, however, the characterization of size varies depending on the measurement method [31].

In the case of static image analysis, the primary size metrics include the projection area of microplastics as well as statistical diameters [52]. From these primary metrics, the area equivalent sphere diameters can be derived. We will now introduce a multitude of statistical diameters, equivalent diameters, and size metrics specifically for fibers, plus provide reasoning for the selection of one of these metrics to routinely characterize the size of microplastics.

Statistical diameters

On digital images, microplastics are represented by their two-dimensional projection, whose size is a function of particle orientation [40]. That is, even for monodisperse particles, their size will distribute around a central value. Therefore, this kind of size metrics are so-called statistical diameters. Although they are named so, they are no diameter in the strict sense. Even for some regular geometries, they do not have the same figure as the diameter.

Statistical diameters are measured by setting a reference point. Depending on which reference point is selected, the result of the particle size measurement is different. For microplastics, Martin's diameter and Feret's diameter have been reported so far [33].

For Martin's diameter, x_M, the reference point is set such that the particle is divided into two halves of equal projection area [40]. Here, the chord length is measured (Fig. 5A).

With Feret's diameter, x_F, one sets any two parallel tangents along the edges of microplastics as a reference point [52]. This approach is similar to the caliper measurement of a real-world particle. Many distinct variants of Feret's diameter can be obtained for an individual microplastic particle (Fig. 5B). The minimum and the maximum Feret's diameter are part of the primary particle size

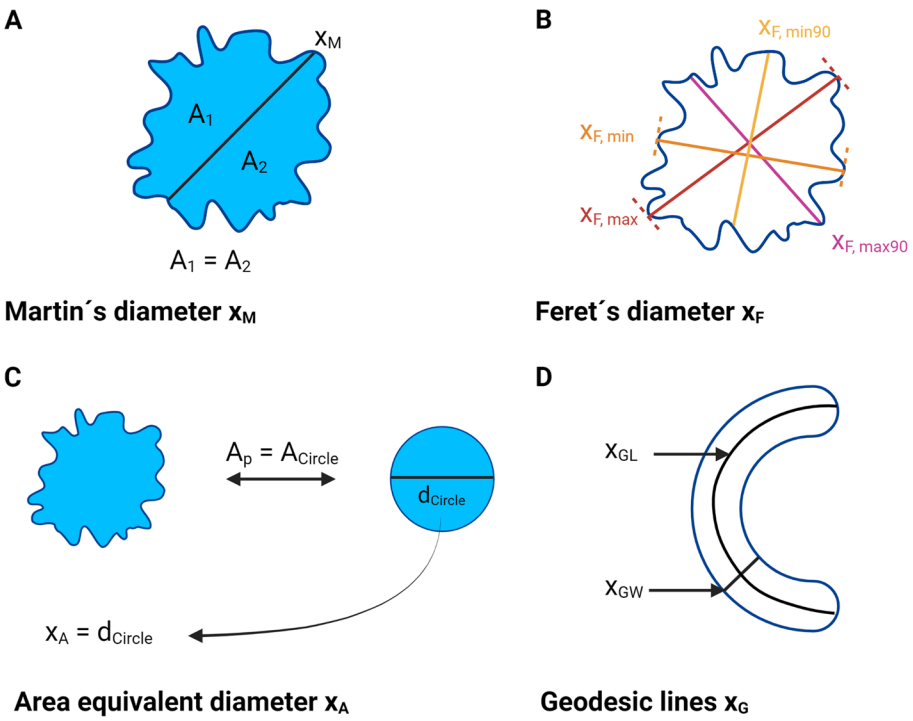

Fig. 5 An overview of the different metrics for characterizing the particle size of microplastics. **A** The Martin's diameter, x_M, is the length of the chord that intersects the projection area into two equally large parts. **B** For Feret's diameter, d_F, a multitude of different types can be defined, e.g., the minimum and maximum Feret's diameter, $x_{F,min}$ and $x_{F,max}$. Additionally, the largest axis perpendicular to these two size metrics is frequently measured as a Feret's diameter ($x_{F,min90}$ and $x_{F,max90}$). The figures of **A** Martin's diameter and **B** Feret's diameter are a function of particle orientation and, consequently, distribute around a central value. That is why they are called statistical diameters. **C** The area equivalent sphere diameter, x_A, is the diameter of a sphere with the same area as the particle under consideration. In the same way an area equivalent square diameter can be measured (not shown). All of the aforementioned size metrics have different figures for a given particle. **D** However, when measuring the size of fibers, they are inappropriate. Instead, the geodesic length, x_{GL}, and width, x_{GW}, should be measured by skeletonizing the two-dimensional projection of microplastics. Overall, the selection of the size metric depends on the research question. Created with biorender.com

measurements [52]. Whereas the minimum Feret's diameter, $x_{F,min}$, characterizes the breadth of microplastics, the maximum Feret's diameter, $x_{F,max}$, is the length of a particle [43]. Length can be alternatively assessed by the largest axis measured at angle of 90 degrees to the the minimum Feret's diameter, $x_{F,min90}$ [43]. In accordance with this, another frequently measured Feret's diameter is the largest axis perpendicular to the maximum Feret's diameter, $x_{F,max90}$. Rosal has proposed to calculate the mean of several Feret's diameters to improve the characterization of particle size for irregular microplastics [33]. However, this calculation must not be done if fibers are present in the particle collective, as mean diameters have no physical meaning for fibers [31].

Note that Feret's diameter tends to be larger than Martin's diameter and the area equivalent sphere diameter [40]. All statistical diameters are generally larger than Stokes diameters, another equivalent sphere diameter [40].

Equivalent diameters

The size of microplastics can also be characterized via the diameter of a simple geometry, e.g., a sphere or a square, which has equivalent properties in relation to a given principle [43]. Considering static image analysis, this principle is the two-dimensional projection area. Thus, the area equivalent sphere diameter, x_A, is defined as the diameter of a sphere with an area equal to the projection area of the plastic particle ([52], Fig. 5C). Its calculation is as follows:

$$x_A = \sqrt{\frac{4A_p}{\pi}} \tag{1}$$

with A_p being the projection area of the particle. As the projection area of microplastics is always been measured in the most stable particle orientation, there is also only one area equivalent sphere diameter for a given particle [43]. This is fundamentally different with statistical diameters, where a large number of values can be obtained. In addition, the area equivalent sphere diameter can be typically measured with greater precision than statistical diameters [43].

From Equation (1) it is possible to directly or indirectly derive other equivalent sphere diameters. The volume equivalent sphere diameter is the diameter of a sphere having the same volume as the plastic particle [43]. From the volume equivalent sphere diameter, both Stoke's diameter and the aerodynamic diameter can then be derived, which are relevant for fate models of microplastics in aquatic environments and the atmosphere, respectively [33]. However, the calculation of these three equivalent diameters is based on moderate or even controversial assumptions [33].

Besides the area, yet another image-based principle is the perimeter and, thus, the size of microplastics can be characterized via a sphere with the same perimeter as the particle. This size metric is termed the perimeter equivalent sphere diameter, x_p. Note that the perimeter is always more prone to digitization errors than the area (c.f. The influence of computer algorithms on shape measurements) and that is why the perimeter equivalent sphere diameter is not a very robust size metric.

Typically, the area equivalent sphere diameter is the largest of all the equivalent sphere diameters [43].

Despite equivalent diameters that uses the sphere as a reference, other geometries can also be utilized as a reference. For instance, the area equivalent square diameter has recently been used to characterize the size of macroplastics [99], but this can also be transferred to microplastics.

$$x_S = \sqrt{A_p}$$

In this equation, A_p is the projection area of the particle. The major advantage of the area equivalent square diameter is that its calculation is very easy.

Geodesic length and width

The size metrics introduced so far can basically be taken for microplastics of all shape categories. However, they do not adequately characterize the size of fibers [100]. For this type of shape, the geodesic length, x_{GL}, and width, x_{GW}, should be measured instead ([100], Fig. 5D).

The geodesic length can be obtained by skeletonizing the two-dimensional projection area of microplastics [36, 101]. This algorithm removes pixels starting from the particles' edge until only the mid-line is left. The number of mid-line pixels from one end to the other is then measured, resulting in the geodesic length. For branched or knotted fibers, the longest length must be found by avoiding any loops. Geodesic width can be characterized either as the minimum, maximum, or mean distance from the mid-line to the edge of the particle [79].

Selection of a size metric

A size metric must be selected for every particle measurement. The selection should be made based on two criteria [43]: Firstly, high-quality data has to be obtained by a simple measurement. Secondly, the size metric should best reflect the properties of interest.

For microplastics, an obvious property is the maximum length, because this defines whether a particle is a microplastic [3, 4]. Hence, it is reasonable to select the maximum Feret's diameter for the characterization of particle size. Its measurement is also rather simple [40] and therefore the maximum Feret's diameter is implemented in

many softwares. Additionally, a high comparability across studies is guaranteed due to frequent reporting in the past [36].

However, a case can be made for other metrics, too. For example, from an ecotoxicological point of view, the minimum Feret's diameter is of importance, as this determines whether an organism can ingest microplastics with its mouth [66].

If a very high accuracy is wished for a particle measurement, then either the area equivalent sphere diameter or the area equivalent square diameter are the most appropriate selection. These size metrics can generally be assessed with a higher accuracy than all of the statistical diameters [43]. This is because the two-dimensional projection area is composed of far more pixels than a straight line, and thus imaging and processing errors bias the measurement to a lesser extent.

A special case are fibers, which is not only the most abundant shape category of environmental microplastics [98], but they also behave quiet different than other particles [33]. Hence, a special analysis of fibers seems to be expedient, which implies the need for a metric that characterizes the size of fibers as accurately as possible, i.e., geodesic length and the maximum geodesic width. Again, the latter is selected by reason that the maximum width is determining whether a species can ingest a particular fiber [66].

However, if different and, thus, incomparable size metrics are measured for the multitude of shape categories, this will likely hinder the application of a unified risk assessment [102]. For this objective, a stable compromise has to be reached. We propose to report the maximum Feret's diameter by default, regardless of the shape category. On the one hand, the maximum Feret's diameter best reflects the way microplastics are defined. On the other hand, for some shape categories, e.g., fibers and films, the size of some particles won't be characterized accurately.

All together, the selection of a representative metric for particle size is not straightforward and ultimately depends on the research question in mind. Of course, this applies not only to each individual study, but also to reviews and meta-analyses that build on these studies. Therefore, it is absolutely advisable to determine a large number of size metrics, even if only one of them is reported (c.f. Step 6: data reporting). The other size metrics should then be made available in the form of open data so that other researchers can select the one that most closely fits their research question [29, 32].

Step 4b: particle shape measurement

The objective of particle shape measurements is to quantify all relevant dimensions of particle shape. For natural sediments, four dimensions have to be characterized, i.e., irregularity, roundness, sphericity, and form [29]. Irregularity refers to the extent of a particles deviation from a regular body [103]. It is the result of convexities and concavities. Roundness describes the sharpness of particle edges. Sphericity is the degree of similarity to a sphere. Lastly, form is the relationship between the three main axes. Form, unlike the other dimensions, cannot be measured directly by static image analysis of two-dimensional projections.

Unfortunately, none of these dimensions exclusively characterizes how much microplastics are stretched out [79, 103]. But the extent of elongation is relevant for the identification of fibers in particle collectives. Thus, in the context of plastic particles, we suggest to characterize shape by the four dimensions of natural sediments together with elongation.

For microplastics, all of these dimensions can best be quantified by shape descriptors [36]. As these are partly named the same as one of the dimensions of particle shape, we italized the name of all shape descriptors.

We are going to provide harmonized equations and interpretations of frequently reported shape descriptors. Subsequently, hierarchical agglomerative clustering is performed to select shape descriptors for characterizing the particle shape of microplastics. Then, we discuss the strong influence of computer algorithms on the accuracy of particle shape measurements.

Shape descriptors

Shape descriptors are defined as size-independent, dimensionless ratios

$$S_{i,j} = \frac{l_i}{l_j} \tag{2}$$

where any shape descriptor $S_{i,j}$ is a function of two different measures, l_i and l_j, of length or length squared [79]. From Equation (2), ten thousands of shape descriptors can be derived, of which about 100 are currently utilized to characterize particle shape [57]. But even with these shape descriptors in use, there is no standardized nomenclature. For this reason, sometimes the same name is assigned to two or more shape descriptors, which, however, are calculated completely differently.

In order to prevent such ambiguities, it is first necessary to set a profile of requirements. According to Crompton, this includes the following three criteria [104]:

- Sensitivity: a shape descriptor must adapt its value to real changes in some aspect of particle shape.
- Intuitivity: the interpretation of their values must be logical and coherent.

- Normalization: the values of a shape descriptor must be between zero and one for easier comparability between studies.

Sensitivity was already proven for microplastics in an experiment with six different plastic types that were treated with mild corrosive chemicals [105]. However, an intuitive interpretation of normalized shape descriptors is usually not yet assured in the case of microplastics. To meet these two criteria, we will now derive equations and interpretations for commonly reported shape descriptors based on the three criteria.

Form factor

Form factor measures the deviation from a perfect sphere by taking into account the smoothness of the perimeter [100].

$$FF = \frac{4\pi A_P}{p_P^2} \tag{3}$$

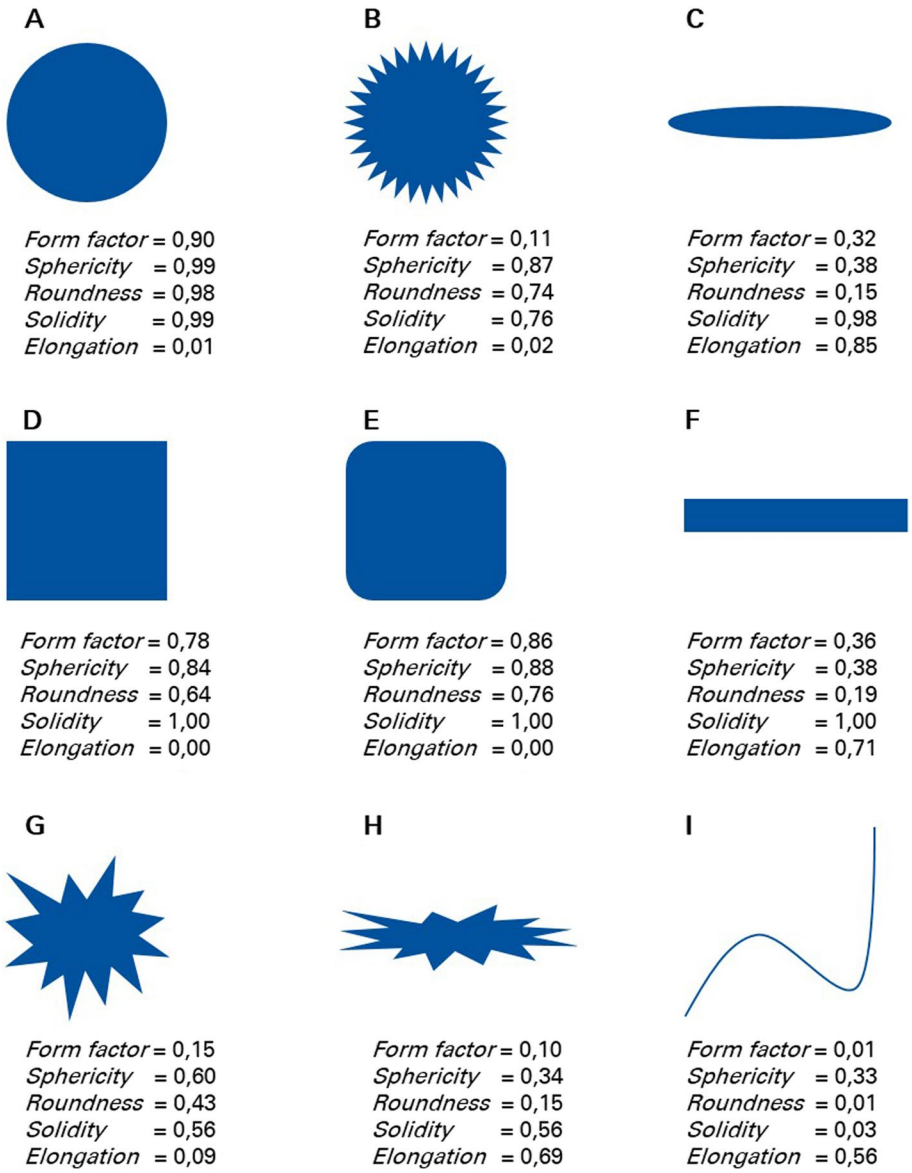

Fig. 6 Values of different shape descriptors for two-dimensional projections of microplastics and some common geometries, i.e., **A** a spherical particle, **B** a spherical particle with rough edges, **C** an ellipse, **D** a quadratic film, **E** a quadratic film with rounded edges, **F** a rectangular film, **G** an irregular particle, **H** a stretched particle with rough edges, and **I** a microfiber

where A_P is the area of the particle and p_P its perimeter. Values close to one refer to an almost perfect spherical particle (Fig. 6A). On the contrary, the *form factor* for rough microplastics is almost zero (Fig. 6B, G, and H).

If the root is taken from Equation (3), one gets the *circularity* of a particle [100]. This popular shape descriptor has also been used to characterize the shape of microplastics. It can be calculated as follows:

$$O = \sqrt{\frac{4\pi A_P}{p_P^2}} \tag{4}$$

However, we prefer the reporting of *form factor*, because this shape descriptor is important for quality control of particle shape measurements [106].

Sphericity

Sphericity measures the deviation of microplastics from a perfect sphere by assessing how fully filled out a particle is [79, 107].

$$P = \sqrt{\frac{r_i}{r_c}} \tag{5}$$

where r_i is the radius of inscribed circle and r_c the radius of the circumscribed circle. *Sphericity* has values close to one for spherical particles (Fig. 6A). For microplastics with large edges, the *sphericity* is much smaller than one (Fig. 6G and H).

Roundness

Roundness is yet another shape descriptor to characterize the deviation from a perfect sphere [79].

$$R = \frac{4A_P}{\pi \cdot x_{F,max}^2} \tag{6}$$

where A_p is the area of the particle, and $x_{F,max}$ its maximum Feret's diameter. For *roundness*, a value close to one have been found if microlastics have a sphere-like appearance ([100], Fig. 6A). Unlike *form factor* and *sphericity*, the *roundness* is different for spheres and rectangular particles. For those shapes, the roundness has intermediate values (Fig. 6D and E).

Solidity

Solidity acts as a measure of particle concavity and is sensitive to changes of the roughness of particle edges [100].

$$S = \frac{A_P}{A_{CH}} \tag{7}$$

where A_P is the area of the particle and A_{CH} the area of the convex hull. In a nutshell, a convex hull could be imagined as a rubber band that is twisted around the particle edges.

Values close to one are measured for microplastics with solid edges (Fig. 6A, C, D, and F). In contrast, the higher the roughness of the particles edges, the closer *solidity* is to zero (Fig. 6B, G, and H).

Elongation

Elongation is a measure of the aspect ratio [33]. It can be calculated as follows:

$$E = 1 - RAR \tag{8}$$

with *RAR* being the *reciprocal aspect ratio*, which is:

$$RAR = \frac{1}{AR} \tag{9}$$

Here, *AR* is the *aspect ratio*:

$$AR = \frac{l}{b} \tag{10}$$

where l is a measure of particle length and b is a measure of particle breadth. Importantly, not a statistical diameter but the geodesic length and width should be utilized to calculate the aspect ratio of very elongated objects like fibers [55, 100].

Values close to one can be found for fibers, while a value close to zero is typical for spherical microplastics (Fig. 6A and I). *Elongation* cannot be used to distinguish between smooth and rough particle edges (Fig. 6F and H).

Both the *reciprocal aspect ratio* and the *aspect ratio* are frequently reported shape descriptors, too [103, 106]. However, they do not comply with the requirement profile by Crompton [104]. Interpreting the *reciprocal aspect ratio* is not intuitive, because a value of one would be determined for spheres and not for microfibers. *Aspect ratio* is not normalized because its values range from 1—∞, with the former being measured for spherical microplastics and the latter for fibers. Therefore, reporting *reciprocal aspect ratio* and *aspect ratio* is not recommended.

Finally, it must be mentioned that none of the shape descriptors we derived here is capable of characterizing all four dimensions of particle shape. This disadvantage can be eliminated by combining several shape descriptors in one equation [108]. However, this method has been criticized because two microplastics with completely different particle shapes can have the same value [109]. Noteworthy, the same criticism also applies to the aforementioned shape descriptors. Thus, these metrics cannot be employed to reconstruct the particle shape [109]. On the one hand, to characterize all four dimensions of

particle shape, reporting multiple shape descriptors is required. On the other hand, it necessitates the selection of non-redundant shape descriptors.

Selection of shape descriptors

To select such a non-redundant subset from the multitude of shape descriptors, we have applied a previously proposed method that combines hierarchical agglomerative clustering and correlation analysis [109]. Here, redundant shape descriptors are first classified into clusters. Within the cluster, the shape descriptor with the highest average correlation coefficient is selected as the representative (c.f. Supplementary Information for details).

The dendrogram showed two branches with a total of three clusters (Fig. 7). The first cluster consisted of the *modification ratio* (Equation S(4)), *form factor*, and *roundness* (Fig. 7). On average, all of these three shape descriptors exhibited a strong positive correlation, with *roundness* being the representative of the first cluster (Table 2). The second cluster was comprised of *R factor* (Equation S(3)), *convexity* (Equation S(2)), and *solidity* (Fig. 7). From these three, *solidity* was the one with the highest average Pearson's r (Table 2). The third cluster was made of *sphericity*, *reciprocal aspect ratio*, and *compactness* (Equation S(1)), Fig. 7). Note that the *reciprocal aspect ratio* is only a placeholder for *elongation*, since the latter does not fulfill the requirements for the cluster analysis *(c.f.* Supplementary Information for details*).* Although compactness exhibited the highest correlation coefficient on average (Table 2), we nonetheless argue against *compactness* as the representative for this cluster. *Compactness* and *roundness* are both sensitive for deviations of a particles' similarity to a sphere [100]. As it would be redundant to select both, *compactness* and *roundness*, we argue for the *reciprocal aspect ratio* and, thus, *elongation* as the representative of the last cluster.

Strikingly, shape descriptors can be selected independent of plastic type and particle size. In dendrograms, which showed the entire size range for each plastic type individually, the clusters were overall very consistent between different plastic types (Fig. S1). The same was observed for different size classes (Fig. S2). In addition, it must be emphasized that different fusion algorithms also had no influence on the clustering (Fig. S3).

The three selected shape descriptors are capable to characterize most of the dimensions of particle shape. *Roundness* is a measure of sphericity, whereas *solidity* can be utilized as an approximation of irregularity. Indeed, *elongation* is a metric that describes elongation. Note that none of the analyzed shape descriptors characterizes roundness. This is due to the fact that, even in the age of digital image processing, measurements of roundness are not trivial due to the ambiguous definitions of particle edges [103]. Consequently, so far no common software offers computer algorithms for the calculation of shape descriptors that has been proposed for the characterization of roundness. These kind of shape descriptors are reviewed elsewhere [103]. Although form cannot be directly assessed from two-dimensional projections, Coreys shape factor can be indirectly calculated by estimating the height of microplastics. This can be done by multiplying the width-to-length ratio by the width [102].

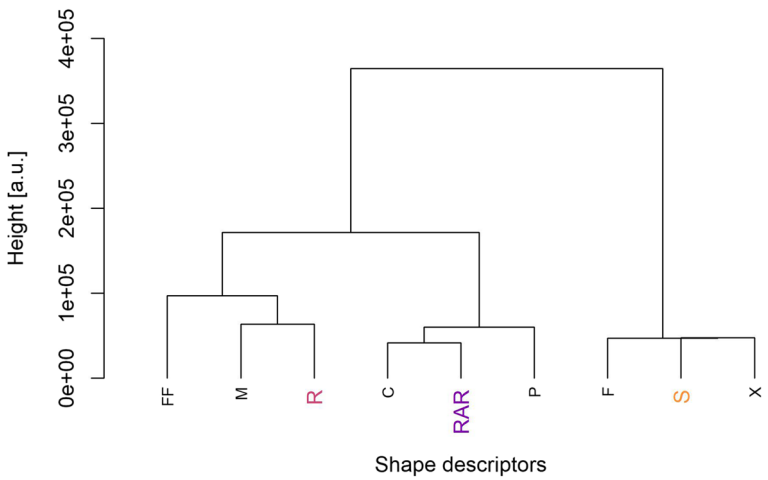

Fig. 7 Dendrogram for the clusters of nine different shape descriptors. The height represents the squared Eucledian distance between individual shape descriptors or clusters, which were formed by hierarchical agglomerative clustering using the centroid fusion algorithm. The color-highlighted shape descriptors are the best representative for the cluster. a.u.: arbitrary unit. *C*: *compactness*. *F*: *R factor*. *FF*: *form factor*. *M*: *modification ratio*. *P*: *sphericity*. *R*: *roundnenss*. *RAR*: *reciprocal aspect ratio*. *S*: *solidity*. *X*: *convexity*

Table 2 Average Pearson's r for each shape descriptor in the respective cluster. The best representatives have been determined by the highest mean correlation coefficient and were highlighted by color

Cluster	Shape descriptor	Mean Pearson´s r
1	*Modification ratio*	0.866
	Form factor	0.834
	Roundness	0.868
2	***Solidity***	0.615
	R factor	0.419
	Convexity	0.473
3	*Compactness*	0.870
	Sphericity	0.820
	Reciprocal aspect ratio	0.821

We are convinced that the default use of the selected shape descriptors will contribute to the much needed harmonization of particle measurements of microplastics. One limitation of our statistical analysis is that the selection of the three shape descriptors from this particular particle collective could hardly be generalized to all microplastics. However, they are at least meaningful for microplastics that are getting produced by milling, as they seem to share some common features [44]. For any other kind of particle collectives, e.g., environmental microplasitcs, the selection of shape descriptors should be performed separately by employing the method that was applied in this review [109].

To assure a high comparability between studies, reporting open data on the main axes as well as the area and the perimeter of both, the plastic particle and its convex hull, should become the new gold standard [29, 32]. This would enable other researchers to calculate the shape descriptors that characterizes their microplastics the best.

Transforming shape descriptors into shape categories

Shape descriptors can be used to classify an individual microplastic particle into one of the shape categories [4, 105]. This method does not only eliminate the observer bias but also enables the development of novel shape categories [105]. A rough classification already exists based on *form factor*: Here, values between 0.0 and 0.3 were measured for films, while values between 0.3 and 0.6 have been found for irregular particles [110]. Values between 0.6 to 1.0 were reported for spherical particles [110]. Fibers can be distinguished from other particle shapes by *aspect ratio* (> 3) or *elongation* (> 0.66) [111]. In addition, microfibers can be distinguished from lines and filaments by *rectangularity* (Eq. (5), [105]). Irregular particles and films are differentiated by *convexity* (Equation

S(2)), whereas pellets can be identified by *compactness* and *roundness*.

Although we advocate for a quantitative characterization of shape, reporting shape categories is helpful in some cases, for instance, regulatory interventions and potential source identification. This highlights that a comprehensive particle measurement facilitates the answer to a wide variety of scientific questions at once.

The influence of computer algorithms on shape measurements

While the calculation of the three selected shape descriptors is mathematically trivial, the accurate measurement of the projection area and especially the perimeter, among other things, is highly dependent on the implementation of robust computer algorithms [79].

The simplest computer algorithm to measure the projection area of microplastics is to count its number of pixels [79]. Likewise, the perimeter is determined by counting the number of sides on the outer margin of pixels.

However, this computer algorithm is prone to digitization errors, as quiet different particle shapes, e.g., a square and a sphere, have the same perimeter, which is obviously incorrect [79]. If such a poor algorithm is applied to measure the perimeter, the value of the *form factor*, and to a lesser extent, *roundness* and *aspect ratio*, becomes size-dependent even for a perfect sphere [79].

For instance, there is evidence that the "Analyze particles" command in ImageJ calculates several shape descriptors incorrectly [106]. This finding is of concern, as the "Analyze particles" command was implemented in software engineered for the identification of environmental microplastics by Nile red staining [86, 110]. A robust alternative is the "Particles8" command of the Morphology plugin [106, 112], which is based on the Freeman algorithm.

With this algorithm, the pixels' center points are getting connected via a line, whose length is equal to the perimeter [113]. The projection area can be measured in a similar manner by measuring the area inside the encompassed projection [113]. Note that this algorithm will result in a smaller area than if pixels are simply counted.

For the calculation of shape descriptors, the aforementioned computer algorithms are often intermixed. Typically, the perimeter is measured by the Freeman algorithm, whereas the area is measured by counting the pixels of the projection [79]. In addition, the application of these computer algorithms have not been not harmonized yet. Especially for very small microplastics, this is problematic, because the value of a shape descriptor is a function of the computer algorithm [100, 106, 114].

That is, calculating the selected shape descriptors by solely using Eqs. (6), (7), and (8) is not sufficient to guarantee a comparable reporting of microplastics shape. Where possible, the very same computer algorithms should be applied to calculate shape descriptors. If this is not possible, the algorithm and the software has to be documented in detail (c.f. Step 3: digital image processing).

In summary, both digitization errors and other errors can potentially worsen the data quality of a particle measurement. It is therefore imperative to be able to take appropriate countermeasures by implementing quality control and quality assurance.

Step 5: quality control and quality assurance

Once the particle measurement of microplastics is completed, it is good laboratory practice to subject the data to quality control and quality assurance (Fig. 1).

This step includes a statistical test for potential outliers in the subsamples, the subtraction of background contamination in the form of dust particles, which have mistakenly entered the microplastic subsamples, the exclusion of microplastics smaller than the practical detection limit of light microscopes, and a validation of the particle shape measurement (Table 5).

Outlier detection in subsamples

Microplastics have to be randomly distributed so that particles in all size intervals can be measured with the same accuracy. However, to achieve this type of mixture, the sampling strategy must be implemented correctly. Otherwise, segregation may bias the median particle size of a subsample, making it an outlier that needs to be detected and replaced.

Outliers can be easily detected by means of null hypothesis significance testing [43]. Several tests have been developed for outlier detection, of which Grubbs's test and Dixon's Q test are suitable in the context of particle measurements. Both tests examine whether either the maximum or the minimum of the subsamples' D_{50} values are an outlier. Note that Grubbs's should not be applied in cases where less than six subsamples were measured [115]. Here, Dixon's Q test serves as a robust alternative. Each of these statistical tests should always be accompanied by diagnostic plots, i.e., histograms and boxplots, to ensure that all outliers have been detected.

If one or more outliers were detected, the particle measurement of the affected subsamples has to be optimized and repeated, followed by yet another check for potential outliers.

Subtracting background contamination

Fine dust from the laboratory environment is a well-documented source of background contamination in microplastic samples [64]. It can substantially bias the lower tail of particle size distributions [42]. Richter and co-workers found that frequencies of microplastics smaller than 50 µm were overestimated by 200—300 particles, whereas size classes larger than 50 µm were less affected by background contamination [42]. Thus, actions are needed to determine the extent of background contamination.

As already called for by other researchers, we recommend to always implement procedural blanks in the workflow, so that the number of non-plastic particles can be estimated via FTIR or Raman spectroscopy. Then, this background contamination can be subtracted from the frequency of microplastics in a given size interval [42].

Such a correction does not only assure an accurate determination of particle size distributions, but also raises the data quality of a static image analysis to the same level as that of the gold-standard, which is laser diffraction [42].

Excluding microplastics smaller than the practical detection limit

Light microscopes can capture images of microplastics down to a size of 1 µm. However, measurements on such small microplastics are only accurate if they are represented by a sufficient number of pixels in a digital image. So what is the practical detection limit of particle measurements?

Theoretically, the lowest uncalibrated size of microplastics on a digital image is one pixel [52]. Of course, the lower the number of pixels, the higher the uncertainty of the measurement, especially for shape descriptors [106].

Thus, the practical detection limit for an accurate particle size measurement by light microscopy is 3 µm [38, 40], whereas microplastics should have a size larger than 10 µm for the calculation of shape descriptors [43].

Ergo, microplastics smaller than these practical detection limits have to be excluded to assure an accurate particle measurement.

Validation of particle shape measurements

In addition to the image resolution, digitization errors caused by segmentation or the computer algorithms used to calculate the shape descriptors influence the accuracy of the particle shape measurement [100]. Hence, the data on shape descriptors needs to be validated prior to reporting.

For this, Kröner & Doménech Carbó [106] proposed a new method that checks whether the measured *elongation* is outside the theoretical range of values for a given value of either *sphericity* or *form factor* (our Equation 3, their *circularity*; Fig. 8). If the measured *elongation* is inside the theoretical value range, the particle shape measurement of the respective microplastic was valid. On the contrary, if the measured *elongation* falls outside the theoretical value range, the shape descriptors are considered to be invalid.

Microplastics with invalid shape descriptors have to be excluded. Their proportion should be given in the data report (Table 3), which is the final step of the particle measurement.

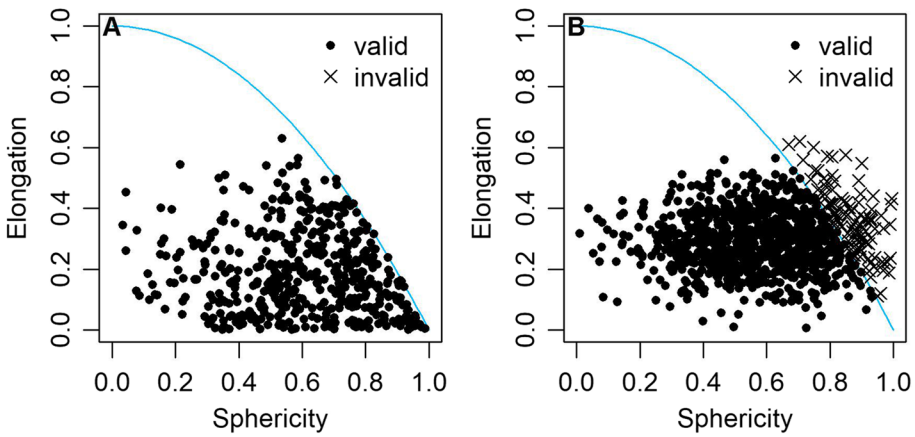

Fig. 8 *Sphericity-Elongation* plots with the solid line representing the maximum *elongation* for a given *sphericity* [106]. **A** For this example, the values of all shape descriptors were in the theoretical range and, thus, the particle shape measurement was considered to be valid. **B** Contrary to the former example, here, the shape descriptors of many microplastics had values outside the theoretical range. Consequently, the particle shape measurement was invalid. To overcome this issue, a more robust computer algorithm should be applied for the determination of shape descriptors. If this does not solve the issue, the image acquisition has to be optimized

Table 3 Items needed for a test report according to ISO 13322–1:2014 [52]

Item	Example
Sample preparation	scooping
Number of subsamples	10
Nominal weigth of subsamples	0.1 mg
Image size	1920 × 1080 pixels
Image resolution	0.44 pixels/µm
Imaging system (hardware & software)	KEYENCE VHX 7000
Type of measurement frame	fully separated measurement frames with microplastics excluded at the image margins
Number of measurement frames	200
Total number of accepted particles	10,000

Step 6: data reporting

The final step of a microplastic particle characterization is to report the measured data in a comprehensive and harmonized format (Fig. 1). The report should comprise a detailed test report [52] as well as particle size distributions [116], frequency density distributions of the selected shape descriptors [100], and summary statistics of both, microplastics' size and shape [117] (Table 5).

Test report

A detailed test report is required for each particle measurement, which is exemplified in Table 3 [52]. In addition, the reporting guidelines for image acquisition and digital image processing should be considered [72, 83]. It is also important to inform the reader on the selection of the size and shape metrics used to characterize the microplastics and the reasoning for this.

Particle size distributions

Particle size distributions show the frequency of microplastics in a given size interval [116]. They have to be accompanied by a representative micrograph of the microplastic particle collective [52].

If particle size distributions are visualized as histograms, there is no general rule for determining the width and the number of size intervals. Generally, the width of size intervals can be either fixed or variable [118]. While fixed size intervals have been reported in the majority of studies, variable size intervals are to be preferred if low particle counts were found at the upper tail of the distribution.

For histograms made of size intervals with a fixed width, one of the oldest and also most frequently applied rules is the formula by Sturges' [119]. It assumes that the data approximately follows a normal distribution, though this is almost never the case with particle size distributions. Accordingly, Sturges' rule should not be applied to assess the number of size intervals. A further development of Sturge's method is Doane's rule [120], which shows good performance also for non-normal distributions. However, this approach tends to oversmooth particle size distributions [118], because of the large sample sizes that are necessary for an accurate particle measurement. Therefore, Doane's rule should be applied with caution. More stringent rules do not estimate the number of size intervals directly, but rather their width. These type of rules are based on a spread parameter of the particle size distribution. The standard deviation is used by Scott's rule [121], whereas the Freedman-Diaconis' rule calculates the width of the size intervals based on the interquartile range [122]. Note that the latter is more robust to extreme values originating from aggregation. Freedman-Diaconis' calculates the width of a size interval, w, as follows:

$$w = \frac{2IQR}{\sqrt[3]{n}} \tag{11}$$

with IQR being the interquartile range, and n the sample size. If the particle size distributions are heavily skewed, then the t-distribution can be used to calculate correction factors for the Freedman-Diaconis' rule [121]. Unfortunately, this correction factor has not been implemented in common statistical software so far. Summing up, the number of size intervals of microplastic particle size distributions with a fixed width can be best estimated by using the Freedman-Diaconis' rule after correction for skewness.

For particle size distributions with size intervals having a variable width, Olson recently derivated a rule for the number of size intervals [118]. Here, the width of the size intervals increases steadily. This means that the size intervals covering small microplastic sizes are less wide than those in the range of large particles. based on a binning constant, c_b:

$$c_b \leq \frac{1.96\sigma}{x_{max}\sqrt{n}} + 1 \tag{12}$$

with σ being the standard deviation, x_{max} the maximum particle size, and, n the sample size. With this binning constant, the number of size intervals, k, can be determined like this:

$$k = \frac{\ln\left(\frac{x_{max}}{x_{min}}\right)}{\ln c_b} \tag{13}$$

where x_{min} and x_{max} are the minimum and maximum particle size. Importantly, the x_{min} should be 10% smaller than the minimum size, whereas x_{max} should be 10% larger than the maximum particle size x_{max}. This ensures that the resulting size intervals cover the whole size range. If variable widths are used to construct the size intervals, it is mandatory to normalize frequencies by dividing them with the width of the size interval [31].

The two formalized rules recommended here can give a first estimate of a suitable number of size intervals. However, care should be taken by researchers to avoid common mistakes in defining the number of size intervals, e.g. oversmoothing [122]. That is, that a continuous distribution turns into a discrete one, a phenomenon that occurs especially in case of histograms with size intervals having a fixed width. Overall, then, the decision on the number of size intervals is a compromise between the desired level of detail and the resolution of the imaging system, the size range, and the width of the particle size distribution, making it a somewhat subjective decision [43].

Care must be taken when histograms are smoothed to curves. The underlying algorithms do not improve the information a given size interval contains in a meaningful manner [43].

What should be avoided at all costs is that too few size intervals are getting reported. Unfortunately, this is often the case microplastics research. For instance, Reinhardt et al. has found that for soil microplastics 86% of all monitoring studies only reported a mean number of four size intervals [60], rendering them ineligible for probabilistic risk modeling [32]. For this, the minimum number of size intervals has to be ten [35]. However, this is still very little, as most definitions consider microplastics to encompass a size range of 1—5000 µm. Thus, scientists have been called on to choose a much higher number of size intervals [32]. However, even then, the information on the size distribution within the size intervals gets lost, but is also relevant for risk assessment [102]. Thus, open data on individual particles should be reported.

Besides their number, two other methodological aspects have to be considered for size intervals. First, we would like to emphasize that it is meaningless to report open size intervals at either one of the tails of a particle size distribution (e.g. < 100 µm or > 1 mm) [31]. Second, closed size intervals should always be right opened [52]. That is, a size interval should contain all microplastics with a size equal to or larger than the lower size limit, and smaller than the upper limit.

Once the number of size intervals has been determined, the frequency of microplastics in each of the size intervals can be calculated. However, calculating unbiased and comparable frequencies is not trivial, as raw frequencies must first be corrected and then normalized [31, 52].

Raw frequency need a correction, because the raw counts itself are almost always biased, if these were obtained by means of static image analysis [52]. When using this method, microplastics that are located on the margins of a measurement frame have to be excluded from particle measurement (c.f. Measurement frames). However, the probability for this exclusion is a function of size: The larger the microplastics, the higher the probability for an exclusion. From this, it also follows logically that the smaller the measurement frame or the higher the frequencies, the larger the potential bias. To correct raw frequencies of microplastics in a given class, a correction factor is first applied to the raw counts of individual microplastics, resulting in their corrected counts, c_c [52]:

$$c_c = c_r \frac{x_{img,h} x_{img,v}}{\left(x_{img,h} - x_{F,h}\right)\left(x_{img,v} - x_{F,v}\right)} \tag{14}$$

with

$$c_r = 1 \tag{15}$$

being the raw count for an individual microplastic particle having a horizontal Feret's diameter of $x_{F,h}$ and a vertical Feret $x_{F,v}$ located inside a measurement frame with a horizontal size of $x_{img,h}$ and a vertical size of $x_{img,v}$. The corrected counts of all microplastics in a given size interval are summed up to obtain the corrected frequency in that interval.

Corrected frequencies have to be normalized for comparability, too. For this, they are simply divided by the width of the size interval, which results in a corrected frequency density [31]. Lastly, these corrected frequency densities are used to construct the histogram.

The axes of the histogram can be visualized either on a linear or a logarithmic scale, depending on the properties of the particle size distribution itself. A logarithmic ordinate should be used whenever corrected frequency densities span several orders of magnitude and only a very low number of particles in the upper size range are present in the sample. Alternatively, size intervals with variable widths can be used to construct the histogram according to Equation (13). Whether the abscissa of a particle size distribution is visualized on a linear or logarithmic scale, depends on its width [43]. It can be classified based on the ratio of D_{90} and D_{10}, which is the 90th and 10th percentile, respectively (Table 4). If the particle size distribution of is very narrow or narrow, its histogram should be shown on a linear scale. In cases where the particle size distribution has a medium to very wide width, a logarithmic representation is favored for the abscissa of the histogram.

Complementary to a histogram, particle size can visualized via a cumulative distribution [116]. From this, frequently reported percentiles of particle size distributions can be easily derived, e.g., D_{10}, D_{50} and D_{90} (Table 4, Summary statistics). It is also common practice to combine the histogram of the corrected frequency density distribution with the cumulative distribution in one graph [43].

Despite methodological questions regarding the construction of a particle size distribution, they are to be reported for each plastic type, each sample site, and each time point separately [102, 123].

Frequency density distributions of shape descriptors

As with particle size, the frequency of shape descriptors depends on the raw counts in a fixed interval, from which either cumulative distributions or a histogram can be constructed [100]. For histograms, most of the methodological guidelines for particle size distributions must be also considered as for shape. To determine how many intervals should be used, the formulas from Equation (11), and (13) can be used on the one hand. On the other hand, a width of 0.1 has been shown to be practical for binning data on shape descriptors [124, 125], resulting in 10 intervals for the selected shape descriptors. Raw frequencies must be normalized with the width of the respective interval to ensure comparability of frequency density distributions between studies [31].

If the size and shape of microplastics are correlated, it may be more informative to visualize shape descriptors as a function of particle size, e.g., as a scatter plot or 2D and 3D density distributions [100, 126].

Table 4 Classification scheme for the width of particle size distributions [43]. It is based on D_{90}/D_{10}, which is the ratio of the 90th and 10th percentile of the particle size distribution. A linear visualization should be preferred for *very narrow* to *narrow* particle size distributions, whereas it is advisable to use a logarithmic scale for particle size distributions with a *medium* to *very wide* width

Width of particle size distribution	D_{90}/D_{10}
Monodisperse	< 1.02 (ideally 1.0)
Very narrow	1.02—1.05
Narrow	1.05—1.5
Medium	1.5—4
Wide	4 – 10
Very wide	> 10

Summary statistics

In addition to distributions, descriptive statistics have to be reported to summarize the data on size and shape.

This can be the parameters of a model, i.e., probability density distributions, which was fitted to the data on particle characteristics [35, 43, 102, 127].

However, most often, a location and spread parameter is calculated for each of the two particle characteristics [117].

As most particle size distributions are heavily left skewed, the mean is not a meaningful location parameter, because it underestimates the central tendency [43]. Instead, mode and median ought to be calculated [43]. In the context of particle measurements, the median is also called D_{50}. While it is standard to specify D_{50} for grain size distributions of natural sediments, it has only rarely been reported for microplastics [29].

The spread of the particle size distributions can be assessed by different statistics [40]. The simplest of these statistics is the range from the maximum to the minimum size. However, this statistic is not robust, since a single agglomerate can easily affect the maximum size. More robust statistics are the inter-quartile range, IQR, and the inter-percentile range between D_{10} and D_{90}, whic are the 90th and 10the percentile, respectively. From these, the D_{90}/D_{10} ratio can also be derived. It is necessary to determine the width of the particle size distribution ([43], Table 4). But the most significant value to characterize the dispersion of microplastics are the standard deviation and the geometric standard deviation [40]. The latter should be reported for log-normal distributed particle sizes, which are typically found for milled microplastics [43].

Summary statistics for shape descriptors comprise either the mean or the median, depending on the skewness of the frequency density distribution. Accordingly, either the standard deviation or the interquartile range should be assessed for the spread.

Conclusions

Measuring the size and shape is not straightforward, but comprehensive and comparable data on these characteristics is essential for the evaluation of the ecological impact of microplastics. To avoid methodological pitfalls in the coming future, we have compiled a practical primer for each of the six steps of a particle measurement (Table 5).

Particularly, we elucidated that the multidimensionality of microplastics can only be characterized using a multitude of metrics, the selection of which depends on the research question. Therefore, reporting of open data on individual microplastics is a must-have [32]. This open data should at least contain the primary

Table 5 Overview of the recommendations for each step of an image-based particle measurement. The time estimates per sample are exemplarily given for around 10,000 microplastics that are used in effect studies. In general, the higher the degree of automation, the faster the method

Step	Time estimate per sample	Aspect	Recommendation
1: Sample preparation	Few hours[a]	Subsampling	Take ten subsamples of equal weight from the homogenized bulk
		Minimum number of particles	300 for environmental microplastics and 10,000 for microplastics that are used in effect studies
		Contamination	Clean instruments and sample holders. Use procedural blanks and avoid plastics. Work with a laminar flow box and cover samples
		De-agglomeration	Sprinkle a small amount of microplastics through a sieve with a mesh size slightly larger than the largest particle
		Measuring points	With effect studies, measure after production, in vivo, and post mortem. For environmental microplastics, measure the filter
2: Image acquisition	1 h – 1 day[a]	Calibration	Calibrate the light microscope by measuring a given distance ten times at different locations on a certified graticule
		Magnification	The magnification should be set so that the smallest particle is represented by at least five to ten pixels in a montage
		Illumination	Always use Köhler illumination. Choose the type of illumination based on the microplastics in the sample
		Depth of focus	Use Z-stacks to maximize the depth of focus
		Image storage	16-bit grey scale images stored as uncompressed.tiff files with all relevant metadata
		Number of field of views	Multiply the minimum number of particles by 5 to 50 particles per field of view
3. Digital image processing	Few seconds (computer vision) – 30 min [128]	Smoothing	Cancel noise by filters. Use them very carefully. Correct uneven illumination a digital image of the empty background
		Contrast	Use auto contrast functions in the whole digital image
		Segmentation	Choose an adequate computer algorithm for global automatic thresholding by qualitative and quantitative comparisons
		Separation of touching particles	Avoid the usage of computer algorithms. Better de-agglomerate the subsamples
4. Measurement	Few seconds (computer vision) [128] – few minutes[a]	Measurement frames	The choice generally depends on the automation of the stage. Neighboring measurement frames can be processed the easiest
		Particle size measurement	Choose a size metric based on the research objective. As a compromise, report the maximum Feret's diameter and open data
		Particle shape measurement	Calculate *roundness*, *solidity*, and *elongation* and provide open data
		Computer algorithms	Measure the perimeter with the Freeman algorithm. Measuring the projection area is done by counting pixels

Table 5 (continued)

Step	Time estimate per sample	Aspect	Recommendation
5. Quality control and quality assurance	1 – 2 days[a]	Outlier detection in subsamples	Apply Grubb's test/Dixon's Q to test whether the extreme values of the subsamples are outliers
		Background contamination	Use procedural blanks to estimate the number of non-plastic particles by spectroscopy
		Excluding of small microplastics	Remove all microplastics < 3 µm from the data analysis
		Validation of particle shape	Use a *Sphericity-Elongation* diagram to detect microplastics with a combination outside the theoretical range
6. Data reporting	Few hours[a]	Test report	Write a test report according to ISO 13322–1:2014
		Particle size distribution	Draw a normalized histogram with corrected counts. Choose the type of visualization (linear/logarithmic) based on the width of the distribution. Alternatively, report a cumulative distribution
		Distributions of shape descriptors	Apply the same recommendations as for particle size distributions. Use a size interval of 0.1
		Summary statistics	Report the median and the (geometric) standard deviation

[a] based on our own experience with 10,000 milled microplastics [124, 125]

particle size measurements, i.e., the maximum Feret's diameter and area, but also perimeter, particle width, and shape descriptors. Reporting these shape descriptors would facilitate addressing many objectives in microplastic research, including theory testing (e.g., shape dissimilarity and shape meditation hypothesis by Rillig and co-workers [37]), fate modelling, risk assessment [26], automatic identification of environmental microplastics [101, 129], effect studies, and the reproducibility of microplastic production by milling. Using particle characteristics to control the quality of a milling in order to produce the same microplastics over and over again becomes especially necessary in the wake of an emerging replication crisis in the environmental sciences [130]. This may also concern microplastics research, making it necessary to critically scrutinize and re-perform previous effect studies with the similar microplastics as the original study.

Not all effects can be related to the size and shape of microplastics [25]. Therefore, other particle characteristics of microplastics need to be considered in risk assessment, too [26]. But even if all of these particle characteristics are routinely measured in the future, many problems with the measurement of microplastics are still unresolved.

First of all, there is the issue of how all of these particle characteristics can be measured under realistic conditions. Suitable methods for particle measurements in environmental matrices have yet to be developed.

Another development, which is of demand for a the comprehensive characterization, are methods for the 3D particle measurement of microplastics [33]. Such a method would allow to directly measure the third principal axis. With this dimension, form could be characterized [29], shapes could be categorized based on 3D shape descriptors [33], and the particle volume could be assessed, which is a prerequisite for studying the fate of microplastics [33] and to convert number concentrations into mass concentrations and vice versa [131].

However, even the best measurement methods have to be validated. For this purpose, reference materials are needed that have the same size, shape, and optical properties as the microplastics to be characterized [52]. Unfortunately, no such reference materials are available at the moment. In their development, a comprehensive particle characterization should be conducted so that measurement methods can be validated.

Furthermore, the computer algorithms to measure the area and perimeter of microplastics must be harmonized. Thus, existing software specifically designed for

the identification of microplastics, e.g., MP-VAT or MP-ACT [110], TUM-ParticleTyper [132], and siMPle [133], should implement the Freeman algorithm for the measurement of area and perimeter.

Computer vision may solve many other problems in the context of particle measurement. Not only does it drastically reduce the processing and measurement times (Table 5), but computer vision also outperforms traditional computer algorithms, which leads to a considerable increase of the accuracy [128]. In addition, microplastics could be easily classified based on particle characteristics [128, 134], which would enable distinct measurements based on different shapes [101]. Although computer vision is a promising tool, more work needs to be done to uncover its full capabilities in microplastic research.

Despite the large number of unsolved problems, by using our practical primer, a robust particle measurement is already possible with the aforementioned trade-offs. A comprehensive characterization should be the standard for any kind of study on microplastics.

Abbreviations

A_{CH}	Area of the convex hull of a particle
A_P	Projection area of a particle
AR	*Aspect ratio*
b	Any measure of particle breadth
c_b	Binning constant for histograms with size intervals having a variable width
c_c	Corrected counts of microplastics within a specific size interval
c_r	Raw counts of microplastics within a specific size interval
D_{10}	The 10th percentile of a cumulative distribution
D_{50}	The 50th percentile (median) of a cumulative distribution
D_{90}	The 90th percentile of a cumulative distribution
D_{90}/D_{10}	Ratio to determine the width of a particle size distribution
E	*Elongation*
FF	*Form factor*
FTIR	Fourier transform infrared spectroscopy
IQR	Interquartile range
JPEG	Joint Photographs Exerpt Group
k	The number of size intervals of a histogram according to Olson's rule
l	Any measure of particle length
LDPE	Low-density polyethylene
l_i	Any metric of particle size
l_j	A metric of particle size other than l_i
n	Sample size
O	*Circularity*
P	*Sphericity*
PBAT	Poly(butylene adipateco- terephthalate)
PBAT/PLA	Blend of PBAT and PLA
PLA	Polylactide
PLA/PBAT	Blend of PLA and PBAT
p_{CH}	Perimeter of the convex hull of a particle
p_P	Perimeter of a particle
R	*Roundness*
RAR	*Reciprocal aspect ratio*
r_i	Radius of the inscribed circle of a particle
r_c	Radius of the circumscribed circle of a particle
S	*Solidity*
$S_{i,j}$	Any 2D shape descriptor derived from two metrics of particle size, l_i and l_j, or size squared
TIFF	Tagged Image File Format
x_A	Area equivalent sphere diameter
x_F	Feret's diameter
$x_{F,h}$	Horizontal Feret's diameter
$x_{F,max}$	Maximum Feret's diameter
$x_{F,max90}$	The length of the largest axis perpendicular to the maximum Feret's diameter
$x_{F,min}$	Minimum Feret's diameter
$x_{F,min90}$	The length of the largest axis perpendicular to the minimum Feret's diameter
$x_{F,v}$	Vertical Feret's diameter
x_{GL}	Geodesic length of fibers
x_{GW}	Geodesic width of fibers
$x_{img,h}$	Horizontal size of an image
$x_{img,v}$	Vertical size of an image
x_M	Martin's diameter
x_{max}	The maximum size of all microplastics in a sample
x_{min}	The minimum size of all microplastics in a sample
x_S	Area equivalent square diameter
w	Width of size intervals in a histogram according to the Freedman-Diaconis rule

Supplementary Information

The online version contains supplementary material available at https://doi.org/10.1186/s43591-023-00064-4.

Additional file 1: Figure 1. Tanglegram for the comparison of the shape descriptor clusters of two distinct size intervals of microplastics. **Figure 2.** Dendrograms for hierarchial agglomerative clustering of shape descriptors for each plastic type individually. **Figure 3.** Dendrograms for hierarchial agglomerative clustering of shape descriptors for different fusion algorithms, i.e., (A) Ward's fusion algorithm, (B) single linkage, and C complete linkage.

Additional file 2.

Acknowledgements
The authors thank Rahma Abdi for her assistance in creating schematic drawings for this manuscript. Thanks are also due to Julia Resch, Christian Bonten and colleagues from the Institut für Kunststofftechnik, Univeristiät Stuttgart, for producing the microplastic that was used for the comparison of computer algorithms.

Authors' contributions
U.S. conceptualized the study; U.S. managed the project, F.B. provided resources; U.S.and M.M. performed the experiments; U.S. and M.M. formally analyzed, interpreted and discussed the results; U.S. and M.M. visualized the data; U.S. curated the data; F.B. was responsible for supervision; U.S. and M.M. wrote the original draft, and all authors reviewed and edited the manuscript.

Funding
Open Access funding enabled and organized by Projekt DEAL. This research is part of the project MiKoBo (Mikrokunststoffe in Komposten und Gärprodukten aus Bioabfallverwertungsanlagen und deren Eintrag in Böden – Erfassen, Bewerten, Vermeiden) in the framework of BWPLUS – Baden-Württemberg Programm Lebensgrundlage Umwelt und ihre Sicherung by the Ministry of the Environment, Climate Protection and the Energy Sector Baden-Württemberg, funded by state funds approved by the state parliament of Baden-Württemberg (reference number: BWMK18002).

Availability of data and materials
The datasets analyzed during the current study are available in the Open Science Framework repository, osf.io/zp963.

Declarations

Ethics approval and consent to participate
Not applicable.

Consent for publication
Not applicable.

Competing interests
The authors declare no competing interests.

Received: 20 April 2023 Accepted: 1 July 2023
Published online: 01 August 2023

References

1. Allen S, Allen D, Karbalaei S, Maselli V, Walker TR. Micro(nano)plastics sources, fate, and effects: what we know after ten years of research. J Hazard Mater Adv. 2022;6:100057.
2. Thompson RC, Olsen Y, Mitchell RP, Davis A, Rowland SJ, John AWG, McGonigle D, Russell AE. Lost at sea: where is all the plastic? Science. 2004;304:838–838.
3. Frias JPGL, Nash R. Microplastics: finding a consensus on the definition. Mar Pollut Bull. 2019;138:145–7.
4. Hartmann NB, Hüffer T, Thompson RC, et al. Are we speaking the same language? Recommendations for a definition and categorization framework for plastic debris. Environ Sci Technol. 2019;53:1039–47.
5. Persson L, Carney Almroth BM, Collins CD, et al. Outside the safe operating space of the planetary boundary for novel entities. Environ Sci Technol. 2022;56:1510–21. https://doi.org/10.1021/acs.est.1c04158.
6. Bank MS, Hansson SV. The plastic cycle: a novel and holistic paradigm for the Anthropocene. Environ Sci Technol. 2019;53:7177–9.
7. Anbumani S, Kakkar P. Ecotoxicological effects of microplastics on biota: a review. Environ Sci Pollut Res. 2018;25:14373–96.
8. Li J, Yu S, Yu Y, Xu M. Effects of microplastics on higher plants: a review. Bull Environ Contam Toxicol. 2022;109:241–65.
9. Shafea L, Yap J, Beriot N, Felde VJMNL, Okoffo ED, Enyoh CE, Peth S. Microplastics in agroecosystems: a review of effects on soil biota and key soil functions. J Plant Nutr Soil Sci. 2022;186:5–22.
10. Prata JC, da Costa JP, Lopes I, Duarte AC, Rocha-Santos T. Environmental exposure to microplastics: an overview on possible human health effects. Sci Total Environ. 2020;702:134455.
11. Royer S-J, Ferrón S, Wilson ST, Karl DM. Production of methane and ethylene from plastic in the environment. PLoS ONE. 2018;13:e0200574.
12. Riveros G, Urrutia H, Araya J, Zagal E, Schoebitz M. Microplastic pollution on the soil and its consequences on the nitrogen cycle: a review. Environ Sci Pollut Res. 2022;29:7997–8011.
13. Stubbins A, Law KL, Muñoz SE, Bianchi TS, Zhu L. Plastics in the Earth system. Science. 2021;373:51–5.
14. Galgani L, Loiselle SA. Plastic pollution impacts on marine carbon biogeochemistry. Environ Pollut. 2021;268:115598.
15. Romera-Castillo C, Pinto M, Langer TM, Álvarez-Salgado XA, Herndl GJ. Dissolved organic carbon leaching from plastics stimulates microbial activity in the ocean. Nat Commun. 2018;9:1430.
16. Wang F, Wang Q, Adams CA, Sun Y, Zhang S. Effects of microplastics on soil properties: current knowledge and future perspectives. J Hazard Mater. 2022;424:127531.
17. Gestoso I, Cacabelos E, Ramalhosa P, Canning-Clode J. Plasticrusts: a new potential threat in the Anthropocene's rocky shores. Sci Total Environ. 2019;687:413–5.
18. Ehlers SM, Ellrich JA. First record of 'plasticrusts' and 'pyroplastic' from the Mediterranean Sea. Mar Pollut Bull. 2020;151:110845.
19. De-la-Torre GE, Dioses-Salinas DC, Pizarro-Ortega CI, Santillán L. New plastic formations in the Anthropocene. Sci Total Environ. 2021;754:142216.
20. Chamas A, Moon H, Zheng J, Qiu Y, Tabassum T, Jang JH, Abu-Omar M, Scott SL, Suh S. Degradation rates of plastics in the environment. ACS Sustain Chem Eng. 2020;8:3494–511.
21. Brümmer F, Schnepf U, Resch J, Jemmali R, Abdi R, Kamel HM, Bonten C, Müller R-W. *In situ* laboratory for plastic degradation in the Red Sea. Sci Rep. 2022;12:11956.
22. Rillig MC, Kim SW, Kim T, Waldman WR. The global plastic toxicity debt. Environ Sci Technol. 2021;55:2717–9.
23. Rivers ML, Gwinnett C, Woodall LC. Quantification is more than counting: actions required to accurately quantify and report isolated marine microplastics. Mar Pollut Bull. 2019;139:100–4.
24. Rochman CM, Brookson C, Bikker J, et al. Rethinking microplastics as a diverse contaminant suite. Environ Toxicol Chem. 2019;38:703–11.
25. Semensatto D, Labuto G, Gerolin CR. The importance of integrating morphological attributes of microplastics: a theoretical discussion to assess environmental impacts. Environ Sci Pollut Res. 2022. https://doi.org/10.1007/s11356-022-24567-4.
26. Koelmans AA, Redondo-Hasselerharm PE, Nor NHM, de Ruijter VN, Mintenig SM, Kooi M. Risk assessment of microplastic particles. Nat Rev Mater. 2022;7:138–52.
27. Bucci K, Rochman CM. Microplastics: a multidimensional contaminant requires a multidimensional framework for assessing risk. Microplastics Nanoplastics. 2022;2:7.
28. Thornton Hampton LM, Bouwmeester H, Brander SM, Coffin S, Cole M, Hermabessiere L, Mehinto AC, Miller E, Rochman CM, Weisberg SB. Research recommendations to better understand the potential health impacts of microplastics to humans and aquatic ecosystems. Micropl&Nanopl. 2022;2:18.
29. Waldschläger K, Brückner MZM, Carney Almroth B, et al. Learning from natural sediments to tackle microplastics challenges: a multidisciplinary perspective. Earth Sci Rev. 2022;228:104021.
30. Thornton Hampton LM, Brander SM, Coffin S, Cole M, Hermabessiere L, Koelmans AA, Rochman CM. Characterizing microplastic hazards: which concentration metrics and particle characteristics are most informative for understanding toxicity in aquatic organisms? Micropl&Nanopl. 2022;2:20.
31. Filella M. Questions of size and numbers in environmental research on microplastics: methodological and conceptual aspects. Environ Chem. 2015;12:527–38.
32. Schnepf U. Realistic risk assessment of soil microplastics is hampered by a lack of eligible data on particle characteristics: a call for higher reporting standards. Environ Sci Technol. 2023;57:3–4.
33. Rosal R. Morphological description of microplastic particles for environmental fate studies. Mar Pollut Bull. 2021;171:112716.
34. Liu F, Rasmussen L, Klemmensen N, Vianello A, Zhao G, Nielsen R, Vollertsen J. The shape of microplastics. In: Abstract Book SETAC Europe 32nd Annual Meeting "Towards a reduced pollution society." Copenhagen: Society of Environmental Toxicology and Chemistry; 2022. p. 320.
35. Kooi M, Koelmans AA. Simplifying microplastic via continuous probability distributions for size, shape, and density. Environ Sci Technol Lett. 2019;6:551–7.
36. Cowger W, Gray A, Christiansen SH, et al. Critical review of processing and classification techniques for images and spectra in microplastic research. Appl Spectrosc. 2020;74:989–1010.
37. Rillig MC, Lehmann A, Ryo M, Bergmann J. Shaping up: Toward considering the shape and form of pollutants. Environ Sci Technol. 2019;53:7925–6.
38. Shekunov BY, Chattopadhyay P, Tong HHY, Chow AHL. Particle size analysis in pharmaceutics: principles, methods and applications. Pharm Res. 2007;24:203–27.
39. Caputo F, Vogel R, Savage J, et al. Measuring particle size distribution and mass concentration of nanoplastics and microplastics: addressing some analytical challenges in the sub-micron size range. J Colloid Interface Sci. 2021;588:401–17.
40. Allen T. Particle size measurement - Volume 1: Powder sampling and particle size measurement. 5th ed. Dordrecht: Springer Dordrecht; 1997.
41. Primpke S, Christiansen SH, Cowger W, et al. Critical assessment of analytical methods for the harmonized and cost-efficient analysis of microplastics. Appl Spectrosc. 2020;74:1012–47.
42. Richter S, Horstmann J, Altmann K, Braun U, Hagendorf C. A reference methodology for microplastic particle size distribution analysis: sampling, filtration and detection by optical microscopy and image processing. Appl Res. 2022. https://doi.org/10.1002/appl.202200055.
43. Merkus HG. Particle size measurements - fundamentals, practice, quality, 1st ed. 2009. https://doi.org/10.1007/978-1-4020-9016-5.
44. von der Esch E, Lanzinger M, Kohles AJ, Schwaferts C, Weisser J, Hofmann T, Glas K, Elsner M, Ivleva NP. Simple generation of suspensible

secondary microplastic reference particles via ultrasound treatment. Front Chem. 2020;8:1–15.
45. Powers KW, Palazuelos M, Moudgil BM, Roberts SM. Characterization of the size, shape, and state of dispersion of nanoparticles for toxicological studies. Nanotoxicology. 2007;1:42–51.
46. Hermsen E, Mintenig SM, Besseling E, Koelmans AA. Quality criteria for the analysis of microplastic in biota samples: a critical review. Environ Sci Technol. 2018;52:10230–40.
47. De Frond H, O'Brien AM, Rochman CM. Representative subsampling methods for the chemical identification of microplastic particles in environmental samples. Chemosphere. 2023;310:136772.
48. Brandt J, Fischer F, Kanaki E, Enders K, Labrenz M, Fischer D. Assessment of subsampling strategies in microspectroscopy of environmental microplastic samples. Front Environ Sci. 2021;8:579676.
49. Schwaferts C, Schwaferts P, Von Der Esch E, Elsner M, Ivleva NP. Which particles to select, and if yes, how many?: Subsampling methods for Raman microspectroscopic analysis of very small microplastic. Anal Bioanal Chem. 2021;413:3625–41.
50. Bucci K, Bikker J, Stevack K, Watson-Leung T, Rochman C. Impacts to Larval Fathead Minnows Vary between Preconsumer and Environmental Microplastics. Enviro Toxic Chem. 2022;41:858–68.
51. International Organization for Standardisation. ISO 14488:2007 Particulate materials - Sampling and sampling splitting for the determination of particulate propertes, 1st ed. Geneva: International Organization for Standardisation; 2007.
52. International Organization for Standardisation. ISO 13322–1:2014 Particle size analysis - Image analysis methods - Part 1: Static image analysis methods, 2nd ed. Geneva: International Organization for Standardisation; 2014.
53. Cabernard L, Roscher L, Lorenz C, Gerdts G, Primpke S. Comparison of Raman and Fourier transform infrared spectroscopy for the quantification of microplastics in the aquatic environment. Environ Sci Technol. 2018;52:13279–88.
54. de Silva RL, Creasy DE. Shape factors for barium chromate crystals in the sieve size range. Powder Technol. 1983;35:181–4.
55. Pons MN, Vivier H, Belaroui K, Bernard-Michel B, Cordier F, Oulhana D, Dodds JA. Particle morphology: from visualisation to measurement. Powder Technol. 1999;103:44–57.
56. Stieß M. Mechanische verfahrenstechnik - partikeltechnologie 1, 3rd ed. 2009. https://doi.org/10.1007/978/3-540-32552-9.
57. Jia X, Garboczi EJ. Advances in shape measurement in the digital world. Particuology. 2016;26:19–31.
58. Souza DOC, Menegalli FC. Image analysis: statistical study of particle size distribution and shape characterization. Powder Technol. 2011;214:57–63.
59. Hidalgo-Ruz V, Gutow L, Thompson RC, Thiel M. Microplastics in the marine environment: a review of the methods used for identification and quantification. Environ Sci Technol. 2012;46:3060–75.
60. Reinhardt I, Schnepf U, Brümmer F. A simplified model for size and shape of microplastics in soil: implications for risk assessment and particle measurement. MICRO 2022, Online Atlas Edition: Plastic Pollution from MACRO to nano. 2022. https://doi.org/10.5281/zenodo.7216859.
61. O'Connor JD, Mahon AM, Ramsperger AFRM, Trotter B, Redondo-Hasselerharm PE, Koelmans AA, Lally HT, Murphy S. Microplastics in freshwater biota: a critical review of isolation, characterization, and assessment methods. Global Chall. 2020;4:1800118.
62. de Ruijter VN, Redondo-Hasselerharm PE, Gouin T, Koelmans AA. Quality criteria for microplastic effect studies in the context of risk assessment: a critical review. Environ Sci Technol. 2020;54:11692–705.
63. Möller JN, Löder MGJ, Laforsch C. Finding microplastics in soils : A review of analytical methods. Environ Sci Technol. 2020;54:2078–90.
64. Dawson AL, Santana MFM, Nelis JLD, Motti CA. Taking control of microplastics data: a comparison of control and blank data correction methods. J Hazard Mater. 2023;443:130218.
65. Eitzen L, Paul S, Braun U, Altmann K, Jekel M, Ruhl AS. The challenge in preparing particle suspensions for aquatic microplastic research. Environ Res. 2019;168:490–5.
66. Horton AA, Svendsen C, Williams RJ, Spurgeon DJ, Lahive E. Large microplastic particles in sediments of tributaries of the River Thames, UK – Abundance, sources and methods for effective quantification. Mar Pollut Bull. 2017;114:218–26.
67. Maxwell SH, Melinda KF, Matthew G. Counterstaining to separate Nile red-stained microplastic particles from terrestrial invertebrate biomass. Environ Sci Technol. 2020;54:5580–8.
68. Nalbone L, Panebianco A, Giarratana F, Russell M. Nile ted staining for detecting microplastics in biota: preliminary evidence. Mar Pollut Bull. 2021;172:112888.
69. Prata JC, Sequeira IF, Monteiro SS, Silva ALP, da Costa JP, Dias-Pereira P, Fernandes AJS, da Costa FM, Duarte AC, Rocha-Santos T. Preparation of biological samples for microplastic identification by Nile red. Sci Total Environ. 2021;783:147065.
70. Schür C, Rist S, Baun A, Mayer P, Hartmann NB, Wagner M. When fluorescence is not a particle: the tissue translocation of microplastics in *Daphnia magna* seems an artifact. Environ Toxicol Chem. 2019;38:1495–503.
71. Möller JN, Heisel I, Satzger A, Vizsolyi EC, Oster SDJ, Agarwal S, Laforsch C, Löder MGJ. Tackling the challenge of extracting microplastics from soils: a protocol to purify soil samples for spectroscopic analysis. Environ Toxicol Chem. 2022;41:844–57.
72. Heddleston JM, Aaron JS, Khuon S, Chew T. A guide to accurate reporting in digital image acquisition – can anyone replicate your microscopy data? J Cell Sci. 2021;134:jcs254144.
73. Kotar S, McNeish R, Murphy-Hagan C, et al. Quantitative assessment of visual microscopy as a tool for microplastic research: Recommendations for improving methods and reporting. Chemosphere. 2022;308:136449.
74. Wolf DE, Samarasekera C, Swedlow JR. Quantitative analysis of digital microscope images. In: Sluder G, Wolf DE editors. Digital Microscopy, 3rd ed. Amsterdam: Academic Press; 2007. p. 365–396.
75. Schäfer M. Digital optics: some remarks on the accuracy of particle image analysis. Part Part Syst Charact. 2002;19:158–68.
76. Zarfl C. Promising techniques and open challenges for microplastic identification and quantification in environmental matrices. Anal Bioanal Chem. 2019;411:3743–56.
77. Clarke J, Gamble JF, Jones JW, Tobyn M, Greenwood R, Ingram A. Alternative approach for defining the particle population requirements for static image analysis based particle characterization methods. Adv Powder Technol. 2019;30:920–9.
78. Podczeck F, Rahman SR, Newton JM. Evaluation of a standardised procedure to assess the shape of pellets using image analysis. Int J Pharm. 1999;192:123–38.
79. Neal FB, Russ JC. Measuring Shape, 1st ed. 2012. https://doi.org/10.1201/b12092.
80. Knop D. Schärfentiefe nach Maß. Biol unserer Zeit. 2019;49:48–57.
81. Burger W, Burge MJ. Digital image processing an algorithmic introduction using java. 2nd ed. 2016. https://doi.org/10.1007/978-3-642-04604-9.
82. Cromey DW. Digital images are data: and should be treated as such. Methods Mol Biol. 2012;931:1–27.
83. Aaron J, Chew T. A guide to accurate reporting in digital image processing – can anyone reproduce your quantitative analysis? J Cell Sci. 2021;134:jcs254151.
84. Uchida S. Image processing and recognition for biological images. Dev Growth Differ. 2013;55:523–49.
85. Rueden CT, Schindelin J, Hiner MC, DeZonia BE, Walter AE, Arena ET, Eliceiri KW. Image J2: imageJ for the next generation of scientific image data. BMC Bioinformatics. 2017;18:529.
86. Erni-Cassola G, Gibson MI, Thompson RC, Christie-Oleza JA. Lost, but found with nile red: a novel method for detecting and quantifying small microplastics (1 mm to 20 µm) in environmental samples. Environ Sci Technol. 2017;51:13641–8.
87. Rossner M, Yamada KM. What's in a picture? The temptation of image manipulation. Eur Sci Edit. 2009;35:35–9.
88. Glasbey CA. An analysis of histogram-based thresholding algorithms. CVGIP Graph Models Image Process. 1993;55:532–7.
89. Doyle W. Operations useful for similarity-invariant pattern recognition. J ACM. 1962;9:259–67.
90. Otsu N. A threshold selection method from gray-level histograms. IEEE Trans Syst Man Cybern. 1979;9:62–6.
91. Brocher J. Qualitative and quantitative evaluation of two new histogram limiting binarization algorithms. Int J Image Process. 2014;8:30–48.

92. Schindelin J, Arganda-Carreras I, Frise E, et al. Fiji: an open-source platform for biological-image analysis. Nat Methods. 2012;9:676–82.
93. Schneider CA, Rasband WS, Eliceiri KW. NIH Image to ImageJ: 25 years of image analysis. Nat Methods. 2012;9:671–5.
94. Narkhede HP. Review of image segmentation techniques. Int J Sci Modern Eng. 2013;1:54–61.
95. Lalitha M, Kiruthiga M, Loganathan C. A survey on image segmentation through clustering algorithm. Int J Sci Res. 2013;2:348–58.
96. Rehman S, Ajmal H, Farooq U, Ain QU, Riaz F, Hassan A. Convolutional neural network based image segmentation: a review. In: Alam MS, editor. Pattern Recognition and Tracking XXIX. Bellingham, Washington: SPIE; 2018. p. 26.
97. Brocher J. BioVoxxel toolbox. 2022. https://doi.org/10.5281/ZENODO.5986129.
98. Li C, Gan Y, Zhang C, He H, Fang J, Wang L, Wang Y, Liu J. "Microplastic communities" in different environments: differences, links, and role of diversity index in source analysis. Water Res. 2021;188:116574.
99. Cowger W, Gray A, Brownlee S, Hapich H, Deshpande A, Waldschläger K. Estimating floating macroplastic flux in the Santa Ana River, California. J Hydrol. 2022;44:101264.
100. International Organization for Standardisation. ISO 9276–6:2008 Representation of results of particle size analysis — Part 6: Descriptive and quantitative representation of particle shape and morphology, 1st ed. Geneva: International Organization for Standardisation; 2008.
101. Primpke SA, Dias P, Gerdts G. Automated identification and quantification of microfibres and microplastics. Anal Methods. 2019;11:2138–47.
102. Kooi M, Primpke S, Mintenig SM, Lorenz C, Gerdts G, Koelmans AA. Characterizing the multidimensionality of microplastics across environmental compartments. Water Res. 2021;202:117429.
103. Blott SJ, Pye K. Particle shape: a review and new methods of characterization and classification. Sedimentology. 2007;55:31–63.
104. Crompton C. Particle shape - an important parameter in pharmaceutical manufacturing. Pharmaceutical Manufacturing and Packing Sourcer. 2005.
105. Valente T, Ventura D, Matiddi M, Sbrana A, Silvestri C, Piermarini R, Jacomini C, Costantini ML. Image processing tools in the study of environmental contamination by microplastics: reliability and perspectives. Environ Sci Pollut Res. 2023;30:298–309.
106. Kröner S, Doménech Carbó MT. Determination of minimum pixel resolution for shape analysis: proposal of a new data validation method for computerized images. Powder Technol. 2013;245:297–313.
107. Riley NA. Projection sphericity. SEPM J Sediment Res. 1941;11:94–5.
108. Podczeck F. A shape factor to assess the shape of particles using image analysis. Powder Technol. 1997;93:47–53.
109. Hentschel ML, Page NW. Selection of descriptors for particle shape characterization. Part Part Syst Charact. 2003;20:25–38.
110. Prata JC, Reis V, Matos JTV, da Costa JP, Duarte AC, Rocha-Santos T. A new approach for routine quantification of microplastics using nile red and automated software (MP-VAT). Sci Total Environ. 2019;690:1277–83.
111. Cole M. A novel method for preparing microplastic fibers. Sci Rep. 2016;6:34519.
112. Landini G. Advanced shape analysis with ImageJ. In: Proceedings of the Second ImageJ User and Developer Conference. Luxembourg: Centre de Recherche Public Henri Tudor; 2008. p. 116–121
113. Freeman H. On the encoding of arbitrary geometric configurations. IEEE Trans Electron Comput EC. 1961;10:260–8.
114. Schroeder S, Braun S, Mueller U, Sonntag R, Jaeger S, Kretzer JP. Particle analysis of shape factors according to American Society for Testing and Materials. J Biomed Mater Res B Appl Biomater. 2020;108:225–33.
115. Adikaram KKLB, Hussein MA, Effenberger M, Becker T. Data transformation technique to improve the outlier detection power of Grubbs' test for data expected to follow linear relation. J Appl Math. 2015;2015:1–9.
116. International Organization for Standardisation. ISO 9276–1:1998 Representation of results of particle size analysis – Part 1: Graphical representation, 2nd ed. Geneva: International Organization for Standardisation; 1998.
117. International Organization for Standardisation. ISO 9276–2:2014 Representation of results of particle size analysis – Part 2: Calculation of average particle sizes/diameters and moments from particle size distributions, 2nd ed. Geneva: International Organization for Standardisation; 2014.
118. Olson E. A study of the effects of histogram binning on the accuracy and precision of particle sizing measurements. Pharm Technol. 2018;42:28–33.
119. Sturges HASR. The choice of a class interval. J Am Stat Assoc. 1926;21:65–6.
120. Doane DP. Aesthetic frequency classifications. Am Stat. 1976;30:181–3.
121. Scott DW. On optimal and data-based histograms. Biometrika. 1979;66:605–10.
122. Freedman D, Diaconis P. On the histogram as a density estimator: L 2 theory. Z Wahrscheinlichkeitstheorie verw Gebiete. 1981;57:453–76.
123. Weber CJ, Bigalke M. Opening space for plastics—Why spatial, soil and land use data are important to understand global soil (micro)plastic pollution. Microplastics. 2022;1:610–26.
124. Schöpfer L, Menzel R, Schnepf U, Ruess L, Marhan S, Brümmer F, Pagel H, Kandeler E. Microplastics effects on reproduction and body length of the soil-dwelling nematode *Caenorhabditis elegans*. Front Environ Sci. 2020;8:41.
125. Schöpfer L, Schnepf U, Marhan S, Brümmer F, Kandeler E, Pagel H. Hydrolyzable microplastics in soil—low biodegradation but formation of a specific microbial habitat? Biol Fertil Soils. 2022;58:471–86.
126. Mukhanov VS, Litvinyuk DA, Evgeniy SG, Bagaev A, Venkatachalapathy V, Venkatachalapathy R. A new method for analyzing microplastic particle size distribution in marine environmental samples. Ecol Montenegrina. 2019;23:77–86.
127. International Organization for Standardisation. ISO 9276–3:2008 Representation of results of particle size analysis - Adjustment of an experimental curve to a reference model, 1st ed. Geneva: International Organization for Standardisation; 2008.
128. Shi B, Patel M, Yu D, et al. Automatic quantification and classification of microplastics in scanning electron micrographs via deep learning. Sci Total Environ. 2022;825:153903.
129. Ismayilova I, Zeyer T, Timpf S. Identification of microplastics in soils using 2D geometric shape descriptors. AGILE. 2021;2:1–6.
130. Deressa T, Stern D, Vangronsveld J, Minx J, Lizin S, Malina R, Bruns S. More than half of statistically significant research findings in the environmental sciences are actually not. 2023. https://doi.org/10.32942/X24G6Z.
131. Koelmans AA, Redondo-Hasselerharm PE, Mohamed Nor NH, Kooi M. Solving the nonalignment of methods and approaches used in microplastic research to consistently characterize risk. Environ Sci Technol. 2020;54:12307–15.
132. von der Esch E, Kohles AJ, Anger PM, Hoppe R, Niessner R, Elsner M, Ivleva NP. TUM-ParticleTyper: a detection and quantification tool for automated analysis of (microplastic) particles and fibers. PLoS ONE. 2020;15:e0234766.
133. Primpke S, Cross RK, Mintenig SM, Simon M, Vianello A, Gerdts G, Vollertsen J. Toward the systematic identification of microplastics in the environment: Evaluation of a new independent software tool (siMPle) for spectroscopic analysis. Appl Spectrosc. 2020;74:1127–38.
134. Massarelli C, Campanale C, Uricchio VF. A handy open-source application based on computer vision and machine learning algorithms to count and classify microplastics. Water. 2021;13:2104.

Publisher's Note

A practical primer for image-based particle measurements in microplastic research

Supplementary Information

Schnepf, Uwe; von Moers-Meßmer, Maria Anna Lioba; Brümmer, Franz

Affiliations

Schnepf, Uwe[1,c] - ORCID: 0000-0003-3955-4484

von Moers-Meßmer, Maria Anna Lioba[1] - ORCID: 0000-0001-5593-3068

Brümmer, Franz[1] - ORCID: 0000-0003-4108-2746

1. University of Stuttgart, Institute of Biomaterials and Biomolecular Systems (IBBS), Research Unit Biodiversity and Scientific Diving, D-Stuttgart, 70569 Germany

c corresponding author: tel.: +49 711 685 64838, email: uwe.schnepf@bio.uni-stuttgart.de

Materials & Methods - Comparison of different algorithms

We examined the influence of segmentation on particle size measurements by using two different software, i.e., FIJI ImageJ 1.53c [1, 2] and the software provided by the manufacturer of a digital microscope (see details below).

For this, microplastics were first produced at the Institut für Kunststofftechnik (University of Stuttgart, Stuttgart, Germany). They were made of the following plastic types: low-density polyethylene without any additives (LDPE; Lupolen 2420 H, LyondellBasell Industries N.V., Rotterdam, Netherlands) and a biodegradable blend of poly(butylene adipate-co-terephthalate) (PBAT; Ecoflex® F Blend C1200, BASF SE, Ludwigshafen, Germany) and poly(lactic acid) (PLA; IngeoTM Biopolymer 7001D, NatureWorks LLC, Minnetonka, MN, United States) (63.5 % PBAT, 10 % PLA, 17 % chalk, 8 % talc, 1% adhesive, 0.5 % anti-blocking agent). The technical data sheets for these plastics can be found below. The PBAT/PLA blend was compounded by extrusion of PBAT and PLA pellets using a twin-screw extruder without using any additives. Frozen pellets (liquid nitrogen, –196 °C) of both plastic types were grinded with a speed rotor mill (Pulverisette, Fritsch GmbH, Idar-Oberstein, Germany). The milled particles were fractionated with stainless steel sieves to obtain the particle size fraction of < 20 µm. The prodcued microplastics were of white color.

Then, the particle characteristics of LDPE and PBAT/PLA were measured via static image analysis [3]. The bulk was mixed for one minute before each of the three subsamples was taken by scooping. Microplastics were then sieved through a

mesh size of 100 µm into clean Petri dishes (diameter 10 cm) to reduce the extent of touching and overlapping particles [4]. They were imaged with a digital microscope by constructing a montage of adjacent Z-stacks (KEYENCE VHX-7000, E20 objective, KEYENCE Deutschland GmbH, Neu-Isenburg, scales: LDPE = 0.453 pixels μm^{-1} and PBAT/PLA = 0.454 pixels μm^{-1}, respectively, image size: 21146 x 21057 pixels – 21157 x 21069).

All images were stored as uncompressed tiff files and digitally processed by either using FIJI ImageJ 1.53c [1, 2] or the software by the microscope manufacturer.

In FIJI ImageJ, microplastics were first segmented by applying the automatic threshold operator developed by Otsu [5]. The processed images were then inspected for erroneously segmented particles by a comparison with the original image. Detected contaminants from the environment were excluded. Particle characteristics were measured by using the Particles8 command (version v2.20) of the Morphology plugin [6].

A comparable method was applied in the software by the manufacturer of the microscope. Unfortunately, the computer algorithm for global automatic thresholding was not verifiable in this case.

For the output of both softwares, the maximum Feret´s diameter was used to characterize particle size of LDPE and PBAT/PLA. This data was analysed by using the statistical software R 4.0.3 [7], RStudio 1.3.1093 [8], plus the packages MPA 1.0.0 [9], and tidyverse 1.3.0 [10]. Artefacts and microplastics smaller than 7 µm were excluded from further analysis [11, 12]. This lower limit of detection was

chosen as a deviation from one pixel would have already corresponded to an error of approximately 33 % at the given scale. Therefore, only particles with a size of four pixels or more were accepted.

Additional shape descriptors

Based on the profile of requirements by Crompton [13], we here introduce equations and interpretation for shape descriptors that have not been discussed in detail in the main text. Except for *rectangularity*, all of these metrics were also considered in the selection of shape descriptors (c.f. Materials & Methods - Selection of shape descriptors).

Compactness is a measure of sphericity and can be calculated as follows [14]:

$$C = \frac{\sqrt{\frac{4}{\pi} * A_P}}{x_{F,max}} \qquad (1)$$

In Equation S(1), A_p is the area of the particle and $x_{F,max}$ its maximum Feret´s diameter. If microplastics have a sphere-like shape, the value of *compactness* is close to one [14].

Convexity assesses the roughness of particle edges. In addition, this shape descriptor was also used to characterize the deviation from a sphere [15]. The following equation was derivatived for the calculation of *convexity* [14]:

$$X = \frac{p_{CH}}{p_P} \qquad (2)$$

Here, p_{CH} is the perimeter of the convex hull, whereas p_P is the perimeter of the particle itself. The rougher the particle edges of microplastics, the larger their perimeter, p_P, and, consequently, the lower the *convexity*. For spherical particles, this shape descriptor has values close to one.

The *R factor* is a shape descriptor that is utilized for the characterization of sphericity and is calculated as follows [6]:

$$F = \frac{p_{CH}}{\pi x_{F,max}} \qquad (3)$$

p_{CH} is the perimeter of the convex hull and $x_{F,max}$ the maximum Feret´s diameter of the respective particle. In cases where microplastics are spherically shaped, the *R factor* approaches one.

Modification ratio is a metric that characterizes both, sphericity and irregularity. The following equation ought to be implemented for its calculation [6]:

$$M = \frac{2r_i}{x_{F,max}} \qquad (4)$$

r_i is the radius of inscribed circle of the particle under consideration and $x_{F,max}$ the maximum Feret´s diameter. The *modification ratio* approaches values close to one for spherical particles. Furthermore, the value of the *modification ratio* decreases if particle edges gets rougher. Note that this shape descriptor cannot be utilized to differentiate between irregular and fibrous microplastics [16].

By the means of *rectangularity*, microfibers can be distinguished from lines and filaments [17]. Therefore, this shape descriptor is relevant in the characterization of microplastics, although it is not in line with the profile of requirements [13]. The *rectangularity* is the product of the particle´s area, A_p, and the area of the bounding box, A_B [6]:

$$Y = \frac{A_P}{A_B} \qquad (5)$$

Here, the area of the bounding box, A_B, is [6]:

$$A_B = x_{F,max} b \qquad (6)$$

The particle breadth, *b*, is characterized via the largest axis perpendicular to the maximum Feret´s diameter, $x_{F,max90}$. The *rectangularity* has a value of zero for cross-like objects, 0.5 for squares, π/4 = 0.79 for circles, and one for long rectangles [6].

Materials & Methods - Selection of shape descriptors

To quantitatively report the particle shape of microplastics in a harmonized way, a selection of non-redundant shape descriptors is required.

Shape descriptors are calculated based on particle size measurements (Equation (2) in the main text) and, thus, redundancies are likely if the size same metrics are used to derive the formulas for different shape descriptors. For instance, *compactness* and *roundness* both describe the similarity to a sphere under consideration of the overall shape with very similar formulas (see Equations S(1) and (6) for comparison). For both shape descriptors, the area of the particle, A_p, and the maximum Feret´s diameter, $x_{F,max}$ are used to characterize the shape of microplastics [14]. It is likely that reporting both, *roundness* and *compactness*, will lead to redundant information on particle shape.

Consequently, the aim of our study was to eliminate such redundancies by applying clustering and correlation analysis to select a minimum number of shape descriptors to quantitatively characterize all dimensions of 2D shape [18, 19].

On behalf of this, we considered data on a wide size range of microplastics made of conventional and biodegradable plastic types: LDPE and PBAT/PLA < 20 µm (this study), LDPE and PLA/PBAT < 50 µm [20], LDPE, PLA and PBAT/PLA in a size range of 50 - 100 µm (this study), plus LDPE and PLA/PBAT either < 500 µm or 500 - 2000 µm [21]. All microlastics were produced by cryo-milling of the same raw material. Overall, 149,781 microplastics sized between 3 and 1960 µm were measured. Notably, the maximum Feret´s diameter as well as eleven different

shape descriptors (Equations (3), (5) - (8) in the main text and S(1) - S(5)) were measured by applying the same computer algorithms [6].

Of these eleven form factors, we had to exclude two (*concavity* and *rectangularity*) from clustering because their value for a spherical particle does not approach one.For the same, in the selection of shape descriptors, *elongation* had to be replaced by *reciprocal aspect ratio* ([22], Equation (9) in the main text). Note that the we also took the square root of the *sphericity* from the Particles_8 command (Equation (5)).

Usually, in cluster analysis, individuals are grouped into clusters based on some variables. Here, we needed to turn the tables. That is, shape descriptors were the individuals, whereas their value for each microplastic was considered as the variable [18].

Therefore, data on all shape descriptors was first transposed and then Z-transformed to a standardized mean of zero and a standard deviation of one [18]. This standardization corrects for different variances between shape descriptors. In addition, a standardization was employed to assure that shape descriptors with inherently larger values do not bias the proximity measure.

For this, the Euclidean distance was chosen since shape descriptors are metrically scaled. Because the aim was to group the shape descriptors, hierarchical clustering was utilized. We further used an agglomerative approach due to the fact that this method considers all individual metrics as a single cluster in the beginning. The centroid fusion algorithm was applied as this incorporates

information from all shape descriptors in a given cluster by only calculating one between-cluster distance [18].

We hypothesized that all shape descriptors can be grouped into three clusters, each of which representing one aspect of 2D particle shape, i.e., shpericity, irregularity, and elongation [19, 22].

The statistical analysis was done with R version 4.2.2 (2022-10-31 ucrt) inside RStudio [7, 8] and the packages tidyverse 1.3.2 [10], data.table 1.14.2 [23], flextable 0.7.3 [24], dendextend 1.16.0 [25], and viridis 0.6.2 [26].

Dendrograms were drawn to illustrate the clusters of shape descriptors. After groups of shape descriptors were identified, one metric had to be chosen as the best representative. Accordingly, Pearson´ r was calculated for each combination of shape descriptors in a cluster [18]. Then, the average Pearson´s r was calculated for each shape descriptor and the shape descriptor with the largest Pearson´s r was selected as the best representative.

Noteworthy, the selection of shape descriptors could possibly be influenced by a variety of parameters, e.g., particle size, plastic type, and the fusion algorithm. Thus, for all of these parameters, we tested whether their consideration would have led to a distinct selection of shape descriptors.

In case of particle size, the data was pooled into two size classes: i) 0 - 500 µm and ii) 500 - 5000 µm. These size classes were inspired by spectroscopic workflows for the identification of environmental microplastics [27]. In particular, for

microplastics in the size range between 0 and 500 µm 148789 particles were examined, whereas 992 microplastics sized between 500 - 5000 µm were analyzed. For each of the two size classes, a dendrogram was constructed. Then, they were combined in a tanglegram for easier comparison (Fig. S1).

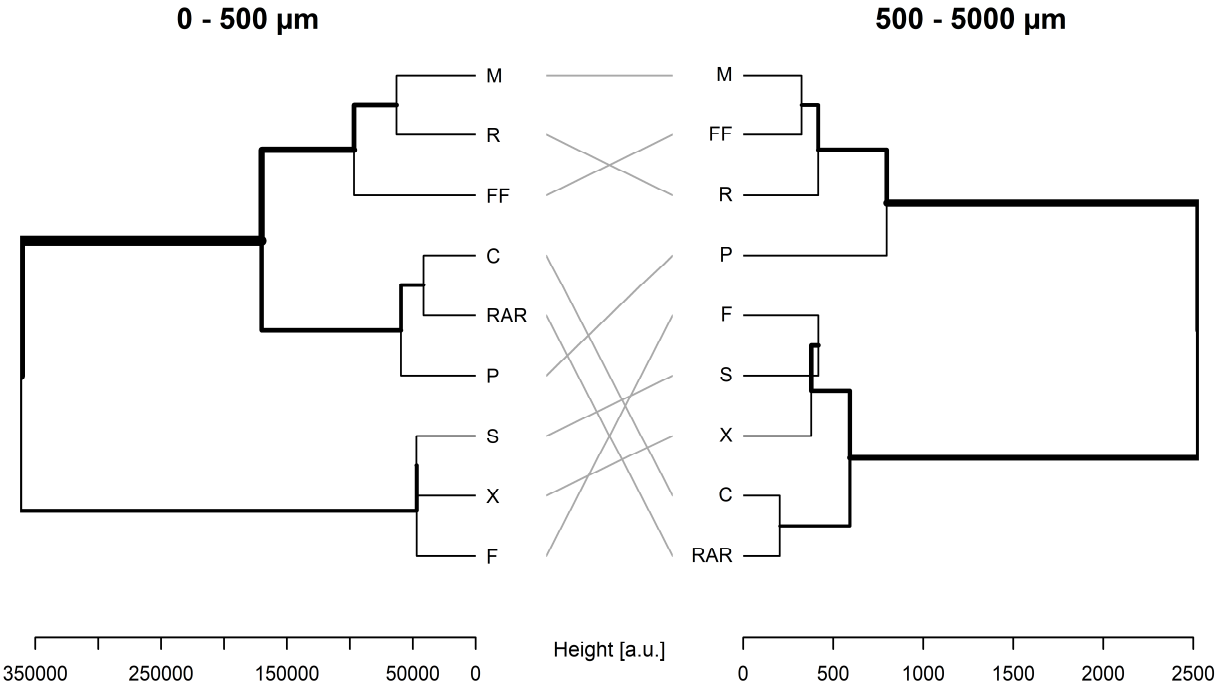

Figure 1: Tanglegram for the comparison of the shape descriptor clusters of two distinct size intervals of microplastics. Standardized Eucledian distance (height) between individual shape descriptors and clusters were hierarchialy agglomerated by the centroid fusion algorithm. a.u.: arbitrary unit. *C*: *compactness*. *F*: *R factor*. *FF*: *form factor*. *M*: *modification ratio*. *P*: *sphericity*. *R*: *roundnenss*. *RAR*: *reciprocal aspect ratio*. *S*: *solidity*. *X*: *convexity*.

Next, we examined whether different plastic types might influence the selection of shape descriptors. Therefore, dendrograms were created for LDPE, PLA,

PLA/PBAT, and PBAT/PLA no matter what their size was (Fig. S2). The subsample of LDPE consisted of 58435 with a D_{50} of 71 µm and a standard deviation of 88 µm. PLA had a median size of 93 µm and a standard deviation of 133 µm, both being measured for 19632 microplastics. By contrast, 16106 and 55608 partilces were characterized for the two blends PLA/PBAT and PBAT/PLA, respectively. The former particle collective had a D_{50} of 31 µm (SD: 117 µm), whereas the latter had a D_{50} of 47 µm (SD: 62 µm).

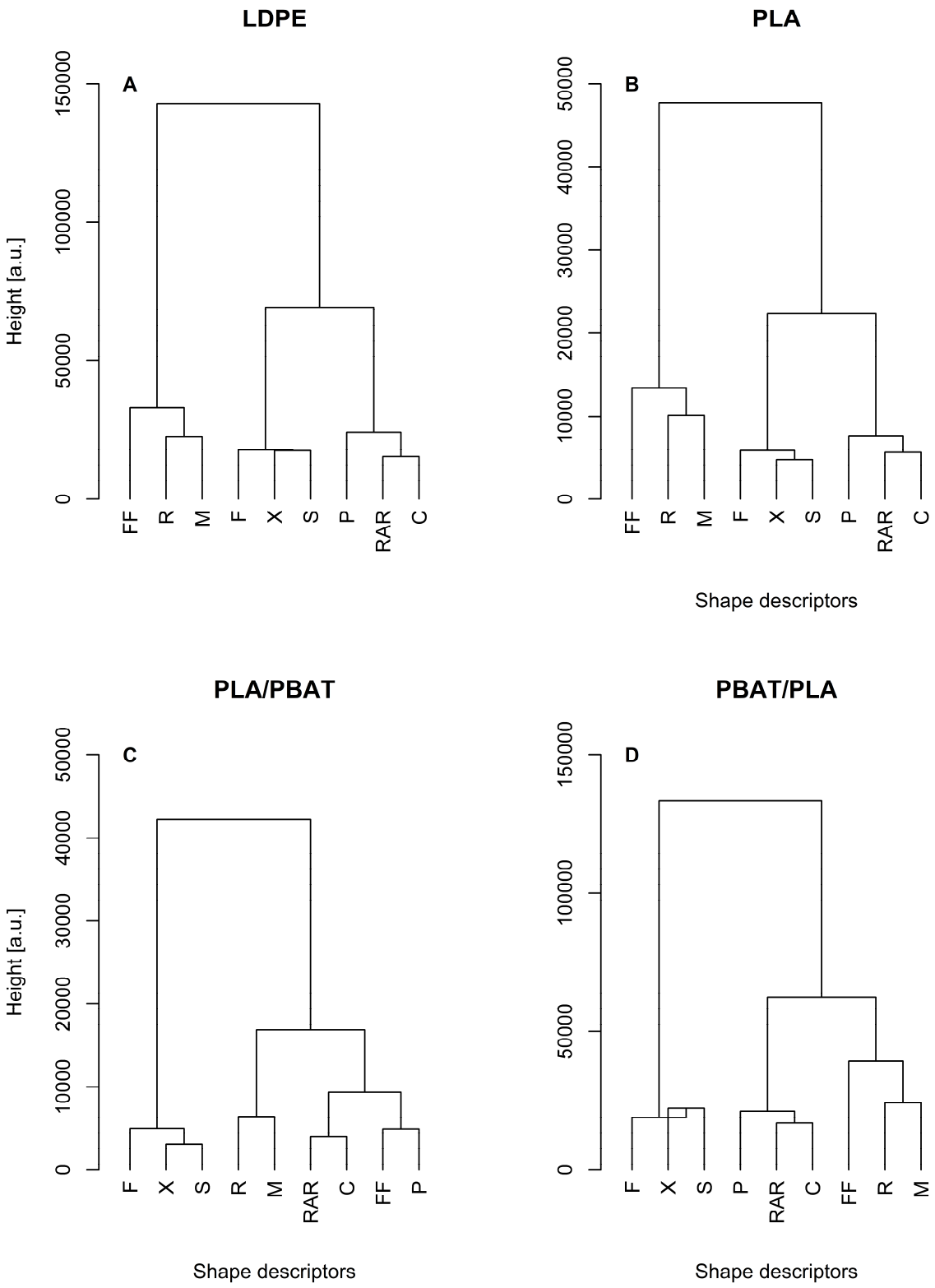
LDPE
A
Height [a.u.]
0
50000
100000
150000
FF
R
M
F
X
S
P
RAR
C
PLA
B
0
10000
20000
30000
40000
50000
Shape descriptors
PLA/PBAT
C
F
X
S
R
M
RAR
C
FF
P
PBAT/PLA
D

Figure 2: Dendrograms for hierarchial agglomerative clustering of shape descriptors for each plastic type individually. (**A**) LDPE. (**B**) PLA. (**C**) PLA/PBAT. (**D**) PBAT/PLA. The height represents standardized Eucledian distance between individual shape descriptors or clusters that were formed by the centroid method. a.u.: arbitrary unit. *C*: *compactness*. *F*: *R factor*. *FF*: *form factor*. *M*: *modification ratio*. *P*: *sphericity*. *R*: *roundnenss*. *RAR*: *reciprocal aspect ratio*. *S*: *solidity*. *X*: *convexity*.

Finally, we tested whether other fusion algorithms could lead to a different selection of shape descriptors. The following fusions algorithms were considered: single linkage, complete linkage, and Ward´s method [28]. For each of these fusion algorithms, a dendrogram was constructed (Fig. S3).

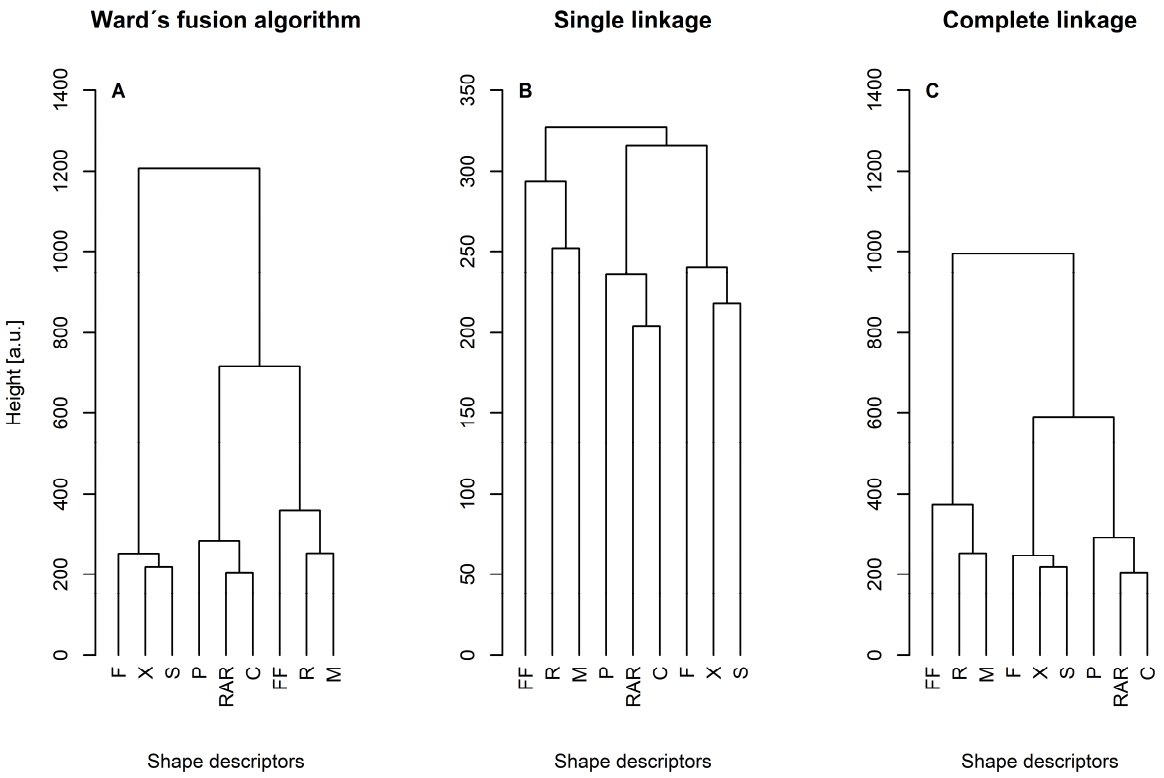

Figure 3: Dendrograms for hierarchial agglomerative clustering of shape descriptors for different fusion algorithms, i.e., (**A**) Ward´s fusion algorithm, (**B**) single linkage, and **C** complete linkage. The height represents standardized Eucledian distance between individual shape descriptors or clusters. a.u.: arbitrary unit. *C*: *compactness*. *F*: *R factor*. *FF*: *form factor*. *M*: *modification ratio*. *P*: *sphericity*. *R*: *roundnenss*. *RAR*: *reciprocal aspect ratio*. *S*: *solidity*. *X*: *convexity*.

List of abbreviations

- A_B: area of the bounding box
- A_{CH}: area of the convex hull of a particle
- A_P: projection area of a particle
- *b*: the particle´s breadth (characterized via the largest measure perpendicular to the maximum Feret´s diameter)
- *C*: *compactness*
- *F*: *R factor*
- LDPE: low-density polyethylene
- *M*: *modification ratio*
- PBAT: poly(butylene adipateco- terephthalate)
- PBAT/PLA: blend of PBAT and PLA
- p_{CH}: perimeter of the convex hull of the particle
- PLA: polylactide
- PLA/PBAT: blend of PLA and PBAT
- p_P: perimeter of a particle
- r_i: radius of the inscribed circle of a particle
- *X*: *convexity*
- $x_{F,max}$: Feret´s diameter
- $x_{F,max90}$: the length of the largest axis perpendicular to the maximum Feret´s diameter
- *Y*: *rectangularity*

References

1. Schindelin J, Arganda-Carreras I, Frise E, et al (2012) Fiji: An open-source platform for biological-image analysis. Nature Methods 9:676–682

2. Schneider CA, Rasband WS, Eliceiri KW (2012) NIH Image to ImageJ: 25 years of image analysis. Nature Methods 9:671–675

3. International Organization for Standardisation (2014) ISO 13322-1:2014 Particle size analysis - Image analysis methods - Part 1: Static image analysis methods, 2nd ed. International Organization for Standardisation

4. Silva RL de, Creasy DE (1983) Shape factors for barium chromate crystals in the sieve size range. Powder Technology 35:181–184

5. Otsu N (1979) A threshold selection method from gray-level histograms. IEEE Transactions on Systems, Man, and Cybernetics 9:62–66

6. Landini G (2008) Advanced shape analysis with ImageJ. In: Proceedings of the Second ImageJ User and Developer Conference. Luxembourg, pp 116–121

7. R Core Team (2021) R: A language and environment for statistical computing.

8. RStudio Team (2016) RStudio: Integrated development for R.

9. Schnepf U (2021) MPA: A R package for data analysis and visualization of particle measurements in microplastic research. https://doi.org/10.5281/zenodo.5027655

10. Wickham H, Averick M, Bryan J, et al (2019) Welcome to the tidyverse. Journal of Open Source Software 4:1686

11. Kröner S, Doménech Carbó MT (2013) Determination of minimum pixel resolution for shape analysis: Proposal of a new data validation method for computerized images. Powder Technology 245:297–313

12. Schäfer M (2002) Digital optics: Some remarks on the accuracy of particle image analysis. Particle & Particle Systems Characterization 19:158–168

13. Crompton C (2005) Particle shape - An important parameter in pharmaceutical manufacturing. Pharmaceutical Manufacturing and Packing Sourcer

14. International Organization for Standardisation (2008) ISO 9276-6:2008 Representation of results of particle size analysis — Part 6: Descriptive and quantitative representation of particle shape and morphology, 1st ed. International Organization for Standardisation

15. Neal FB, Russ JC (2012) Measuring Shape, 1st ed. https://doi.org/10.1201/b12092

16. Mikli V, Kaerdi H, Kulu P, Besterci M (2001) Characterization of powder particle morphology. Proceedings of the Estonian Academy of Sciences: Engineering (Estonia) 7:22–34

17. Valente T, Ventura D, Matiddi M, Sbrana A, Silvestri C, Piermarini R, Jacomini C, Costantini ML (2023) Image processing tools in the study of environmental contamination by microplastics: Reliability and perspectives. Environmental Science and Pollution Research 30:298–309

18. Hentschel ML, Page NW (2003) Selection of descriptors for particle shape characterization. Particle & Particle Systems Characterization 20:25–38

19. Waldschläger K, Brückner MZM, Carney Almroth B, et al (2022) Learning from natural sediments to tackle microplastics challenges: A multidisciplinary perspective. Earth-Science Reviews 228:104021

20. Schöpfer L, Menzel R, Schnepf U, Ruess L, Marhan S, Brümmer F, Pagel H, Kandeler E (2020) Microplastics effects on reproduction and body length of the soil-dwelling nematode *Caenorhabditis elegans*. Frontiers in Environmental Science 8:41

21. Schöpfer L, Schnepf U, Marhan S, Brümmer F, Kandeler E, Pagel H (2022) Hydrolyzable microplastics in soil—low biodegradation but formation of a specific microbial habitat? Biology and Fertility of Soils 58:471–486

22. Blott SJ, Pye K (2007) Particle shape: A review and new methods of characterization and classification. Sedimentology 55:31–63

23. Dowle M, Srinivasan A (2021) Data.table: Extension of 'data.frame'.

24. Gohel D (2021) Flextable: Functions for tabular reporting.

25. Galili T (2015) Dendextend: An R package for visualizing, adjusting and comparing trees of hierarchical clustering. Bioinformatics 31:3718–3720

26. Garnier S (2018) Viridis: Default color maps from 'matplotlib'.

27. Möller JN, Löder MGJ, Laforsch C (2020) Finding microplastics in soils : A review of analytical methods. Environmental Science & Technology 54:2078–2090

28. Backhaus K, Erichson B, Plinke W, Weiber R (2018) Multivariate Analysemethoden: Eine anwendungsorientierte Einführung. https://doi.org/10.1007/978-3-662-56655-8